SURFACE ADSORPTION OF HYDROXYAPATITE NANOPARTICLES WITH CATECHOL MODIFIED HYALURONIC ACID

by

Nihan Ataalp

B.S, Chemistry, Yıldız Technical University, 2009

Submitted to the Institute for Graduate Studies in
Science and Engineering in partial fulfillment of
the requirements for the degree of
Master of Science

Graduate Program in Chemistry

Boğaziçi University

2016

SURFACE ADSORPTION OF HYDROXYAPATITE NANOPARTICLES WITH CATECHOL MODIFIED HYALURONIC ACID

APPROVED BY:

Assist. Prof. A. Başak Kayıtmazer ..…….

Assist. Prof. Bülent Akgün …….

Prof. Sabri Altıntaş …….

DATE OF APPROVAL: 17.05.2016

ACKNOWLEDGEMENTS

I would like to express my deepest gratitude to my thesis advisor Assist. Prof. A. Başak Kayıtmazer for her support, endless patience and assistance throughout my studies. Everything I have learned about scientific research is thanks to her. There is no words to thank her enough for giving me the opportunity to work in this project and being always available whenever I need guidance.

I would like to thank the members of my committee: Assist. Prof. Bülent Akgün and Prof. Sabri Altıntaş for giving their valuable time in reviewing this thesis and for all the advices.

I would also like to thank Dr. Bilge Gedik Uluocak for Scanning Electron Microscopy and Dynamic Light Scattering analysis.

I thank to all members of Kayıtmazer Research Group, Alaaddin Faruk Köksal, Pınar Ansen for their help in my research and especially to Fatih Çömert for his additional support and friendship. I must express my greatfulness to İpek Gümüş, Sümeyye Gündüz, Murat Can Keklik and Savaş Demiray for their endless friendship, support and valuable discussions. I would also like to thank all my friends, colleagues and all the members of the Chemistry Department.

Finally, my deepest thanks are for my dear family. They have always been there with their loving hearts and endless support whenever I needed.

This research has been supported in part by grant by Bogazici University Research Fund (5684) and European Union 7th Framework Marie Curie International Reintegration Grant (BONEMIM256498).

ABSTRACT

SURFACE ADSORPTION OF HYDROXYAPATITE NANOPARTICLES WITH CATECHOL MODIFIED HYALURONIC ACID

Biopolyelectrolytes have been a very popular research field due to their applications ranging from food science to biomaterials. Biopolyelectrolytes can bind with higher affinity to the surfaces of biodevices if their structure is modified with various chemical groups. In the long term, the goal here was to prepare artifical bone. In the short term, our goal was to prepare systems where biopolyelectrolytes are adsorbed onto hydroxyapatite nanoparticles.

In this study, at the first step, the effects of 2-carboxyethyl phosphonic acid (CEPA) and citrate on the synthesis of hydroxyapatite nanoparticles were investigated. In another method, hydroxapatite nanoparticles were synthesized while controlling crystallinity. In the next step, hydroxyapatite adsorption of polyacrylic acid (PAA), unfunctionalized HYA (hyaluronic acid) and catechol functionalized HYA were compared. Fourier Transform Infrared spectroscopy (FTIR) and thermogravity analysis (TGA) were applied to characterize the samples. According to the TGA characterization results, the highest level of surface modification on hydroxyapatite nanoparticles (3.25 %) was found for catechol functionalized hyaluronic acid (234 kDa).

ÖZET

HİDROKSİAPATİTİN KATEKOL MODİFİYELİ HYALURONİK ASİT İLE YÜZEY ADSORPSİYONU

Biyopolielektrolitler, gıda biliminden biyomalzemelere uzanan uygulamaları ile son yıllarda oldukça populer bir çalışma alanı olmuştur. Biyopolielektrolitlerin biyocihaz yüzeylerine iyi bir afinitede bağlanabilmesi çeşitli kimyasal gruplar yardımı ile istenilen özellikler doğrultusunda modifikasyonları sayesinde mümkündür. Uzun vadede, yapay kemik üretiminde kullanılmak üzere biyopolielektrolitlerin hidroksiapatit nanopartiküllerine fiziksel adsorpsiyonla bağlı olduğu sistemler elde edilmesi amaçlanmaktadır.

Bu çalışmada ilk aşamada 2-karboksietil fosforik asit ve sitrat ile muamelenin hidroksiapatit nanopartikül sentezindeki etkisine bakılmıştır. Bir diğer yöntemde ise kristal yapıyı kontrol altında tutarak kalsiyum fosfat nanopartikülleri sentezlenmiştir. Bir sonraki aşamada ise modifiye edilmemiş poliakrilik asit ve hiyalüronik asit ile katekol gruplarıyla modifiye edilmiş hiyalüronik asidin hidroksiapatit nanopartikülleri üzerine adsorpsiyonları karşılaştırılmıştır. Elde edilen örneklerin Fourier Transform Infrared spektroskopisi ve termogravimetrik analiz yöntemleri ile karakterizasyonları yapılmıştır. Sonuçlara göre, hidroksiapatit nanopartiküllerine en yüksek yüzey adsorpsiyon oranı % 3.25 ile katekol modifikasyonuna uğramış yüksek moleküler ağırlıktaki hiyalüronik asit (234 kDa) ile sağlanmıştır.

TABLE OF CONTENTS

LIST OF FIGURES

LIST OF TABLES

LIST OF ACRONYMS / ABBREVIATIONS

ACP	Amorphous Calcium Phosphate
CEPA	2-Carboxyethyl phosphonic acid
DCP	Dicalcium Phosphate
DTA/TG	Differential Thermal Analysis/Thermogravimetric
FTIR	Fourier Transform Infrared Spectroscopy
HAP	Hydroxyapatite
HYA	Hyaluronic acid
PAA	Polyacrylic acid
SEM	Scanning Electron Microscopy
SIAL	Sigma Aldrich
TGA	Thermogravimetric Analysis
TTCP	Tetracalcium Phosphate
XRD	X-Ray Diffraction
α-TCP	Alpha-tricalcium Phosphate
β-TCP	Beta- tricalcium Phosphate

1. INTRODUCTION

1.1. Bone Material

1.1.1. Structure and Composition of Bone

Human skeleton has a remarkable structure with many uses such as protection of internal organs (live, lung, heart etc.), deposition of minerals like calcium and phosphorus, and assisting mobility via joining muscles. Bone, as a main connective tissue, consists of the trabecular and cortical bone [1].

Bone consists of 35 wt % of organic minerals, 65 wt % of inorganic compounds and 10 wt % of water [2]. Bone also contains a small amount (5 wt %) of other proteins and inorganic salts (Table 1) [4]. Collagen is a nucleation site for the bone mineral crystals. On the other hand, calcium phosphate gives the stiffness to the bone. Calcium phosphate can be present as crystallized hydroxyapatite and/or amorphous calcium phosphate [1].

Table 1.1. Composition of inorganic phases of bone versus synthetic hydroxyapatite [4]

Composition wt %	Bone	Hydroxyapatite
Ca/P (molar ratio)	1.71	1.67
Sodium	0.9	-
Magnesium	0.72	-
Potassium	0.03	-
Carbonate	7.4	-
Fluoride	0.03	-
Chloride	0.13	-
Pyrophosphate	0.07	-
Water	10	-

1.1.2. Calcium Phosphate Minerals

The main inorganic component of bone is calcium phosphate. Chemically, calcium phosphate is composed of carbonated hydroxyapatite, $(Ca,X)_{10}(PO_4,HPO_4,CO_3)_6(OH,Y)_2$, for which X can be magnesium, sodium or strontium ions while Y can be chloride or fluoride [5].

The molar ratio of Ca to P in bones is between 1.00 and 2.00 according to the properties (species, age, type) of bone. The ratio is mostly above 1.67 for pure HAP as can be seen in Table 1.1 [2].

These inorganic minerals, i.e. calcium phosphates, are irregularly shaped platelets (30 - 45 nm wide and ~5 nm thick), which are parallel to each other with respect to the c axis and are located throughout the length of the collagen fibrils (Figure 1.1 and 1.2) [2].

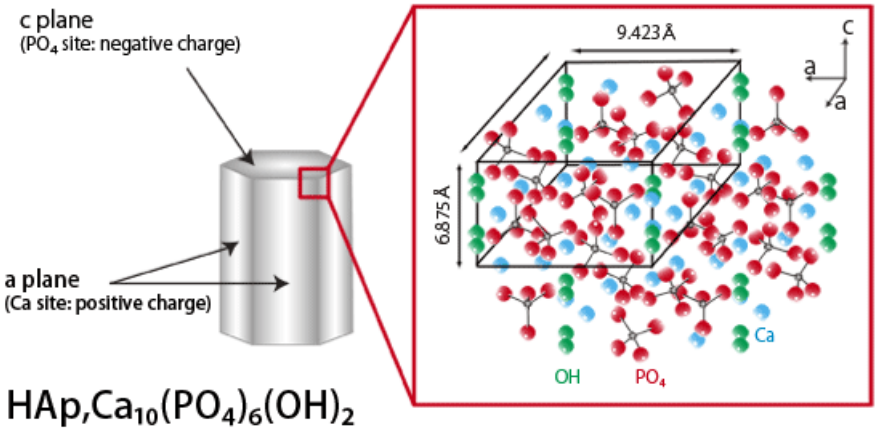

Figure 1.1. Atomic structure of hydroxyapatite in details [6]

Based on the composition, commercial calcium phosphate biomaterials have different classifications; hydroxyapatite, tricalcium phosphate ($Ca_3(PO_4)_2$), biphasic calcium phosphate, and unsintered CaP or a calcium deficient apatite $(Ca,Na)_{10}(PO_4\ HPO_4)_6(OH)_2$). The solubility of these types of different calcium phosphates depends on their formation and stoichiometry. The order of solubility is as follows: ACP > DCP > TTCP > α-TCP > β-TCP >> HAP [5].

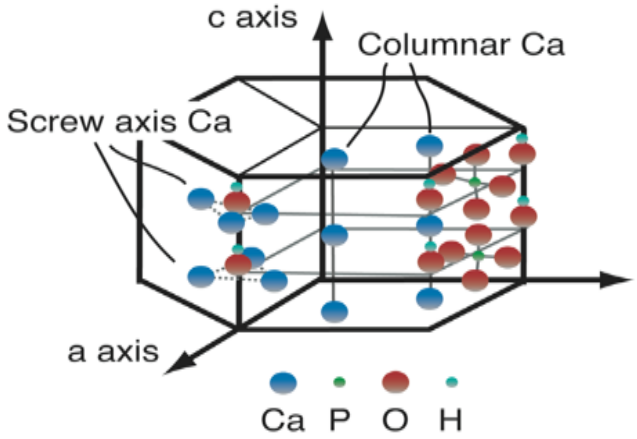

Figure 1.2. Hydroxyapatite crystal structure
(Available from [7])

Calcium phosphate nanoparticles are biocompatible and biodegradable. They are also easily functionalized. In spite of the many open questions about the medical applications of nanoparticles, calcium phosphate nanoparticles have been used in many applications such as transfection [8], drug delivery [9], dental cements [10], gene silencing [11], transportation of photosensitizers [12] and polymers for photodynamic therapy against cells and bacteria [13].

Besides these applications, especially in the past two decades, calcium phosphate biomaterials have been highlighted in orthopedic applications. In 1920, the first successful repair of a bone with a calcium phosphate material was reported by Albee [14]. The second orthopedic application was reported 30 years later by LeGeros [15].

1.2. Hydroxyapatite

1.2.1. Definition and Chemical Structure

Hydroxyapatite (usually written as $Ca_{10}(PO_4)_6(OH)_2$) with a stoichiometric Ca/P molar ratio of 1.67, is the primary mineral of teeth and bones. Although it would be more correct to name it as hydroxylapatite, the common name known within the medical and

material researchers is hydroxyapatite [1]. The following compounds given in Table 1.2 are intermediate during the formation of hydroxyapatite [16].

Table 1.2. Intermediate compounds before Hydroxyapatite forms [16]

Name	Abbreviation	Ca/P
Hydroxyapatite	HAP	1.67
Carbonated hydroxyapatite	CHA	1.67
Fluorapatite	FHA	1.53
α-β tricalcium phosphate	α-β-TCP	1.55
Amorphous calcium phosphate	ACP	1.55
Octacalcium	OCP	1.33

The hydroxyapatite crystals are stored parallel to the collagen fibers in bones. These crystals are "about 40–60 nm long, 20 nm wide, 1.5–5 nm thick" and are in the form of plates or needles [17]. The structure of hydroxyapatite was described by Posner and Betts, who emphasized that aggregates were formed by accumulation of $Ca_9(PO_4)_6$ clusters [18]. While hydroxide can be replaced with other ions (such as fluorine and chlorine ions), this is also the reason of not observing the exact 1.67 molar ratio in some organisms [19].

Commercial hydroxyapatite has two types based on the derivation from coral-sources or bovine bone sources. Whereas coral-derived hydroxyapatite (also called as coralline hydroxyapatite) consists of CO_3, Mg, Sr, and F, bovine bone-derived hydroxyapatite consists of CO_3, Mg, Na as minor elements [20].

1.2.2. Chemical and Mechanical Properties

Hydroxyapatite has many properties: it is bioactive, osteoconductive, non-toxic, non-immunogenic. Besides these properties, the best feature of hydroxyapatite is its ability to directly bond to the bone [1].

Due to its stability at pH's above 4.2, hydroxyapatite is the least soluble calcium phosphate compound. But this solubility can be changed with the substitutions. For example, Mg, Sr, CO_3 increases the solubility while F decreases it in comparison with the unsubstituted compounds [1].

As for the mechanical properties (Figure 1.3), hydroxyapatite is limited in medical applications because of its poor mechanical properties. However, hydroxyapatite-containing composites or nanometer-size crystallines may be a solution to overcome this disadvantage [21]. Especially, due to the nano size, hydroxyapatite can have large interfaces, great adsorption capability and high catalytic activity [19].

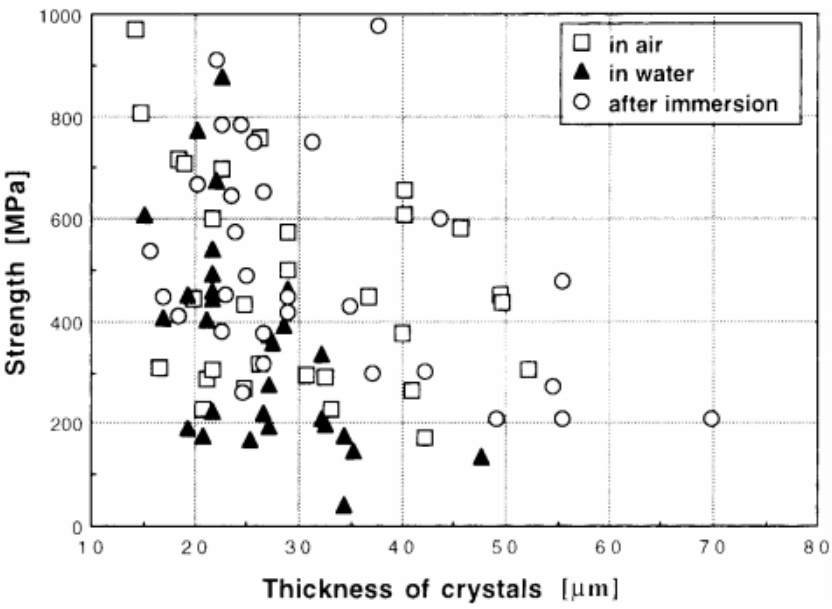

Figure 1.3. Bending strength versus crystal thickness in air, in water and after immersion [21]

1.2.3. Synthesis Methods

Preparation methods of hydroxyapatite can mainly be divided into two classes; i.e. solid-state reactions and wet methods. The most known methods are precipitation, microemulsion, hydrothermal and sol-gel method [1]. Table 1.3 summarizes the preparation of HAP nanoparticles with strong and weak features of those methods [22].

Table 1.3. Methods for preparation of HAP nanoparticles and the results of characterization of these nanoparticles [22]

Method		**Characteristics of powder**			
		Morphology	**Phase purity**	**Ca/P ratio**	**Size**
Dry methods	Solid state method	Diverse	usually low	Variable	usually micron
	Mechano chemical method	Diverse	low	usually non-stoichiometric	Nano
Wet methods	Chemical precipitation	diverse	varia-ble	non-stoichiometric	usually nano
	Hydrolysis method	diverse	usually high	stoichiometric	variable
	Sol-gel method	diverse	varia-ble	stoichiometric	nano
	Hydrothermal method	frequently needle-like	usually high	stoichiometric	nano or micron
	Emulsion	frequently needle-like	varia-ble	non-stoichiometric	nano
	Sonochemical method	diverse nee-dle-like	usually high	variable	nano

1.2.4. Characterization

Various characterization methods are used to observe the morphologies of hydroxyapatite crystals to determine size/diameter of crystals, chemical/ionic groups of particles/powders and also to investigate formation of the new bone as shown in the examples of analysis below.

X-Ray Diffraction (XRD) demonstrates crystallinity of hydroxyapatite as shown in Fig 1.4. Additionally, the size and morphology of synthesized HAP powders or particles is evaluated with XRD data [23].

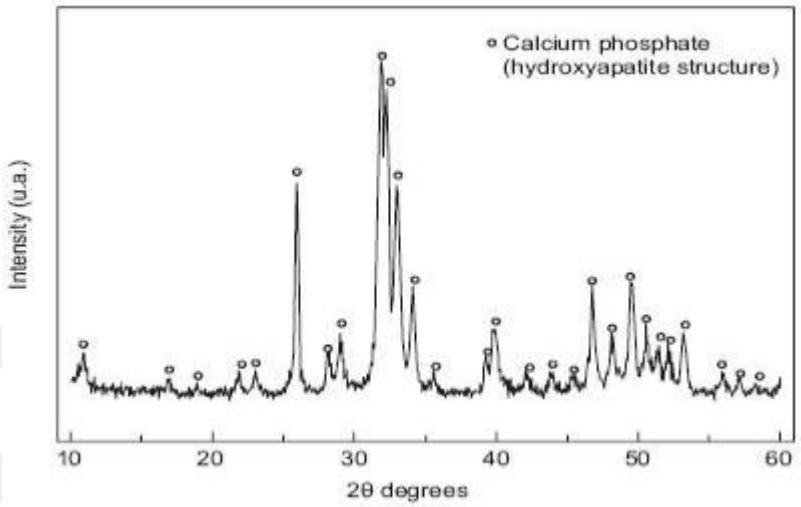

Figure 1.4. XRD pattern of hydroxyapatite (Reprinted with permission from Posner, A.S. and F. Betts, Synthetic amorphous calcium phosphate and its relation to bone mineral structure. Accounts of Chemical Research, 1975. 8(8): p. 273-281. Copyright 2016 American Chemical Society) [17]

Furthermore, the crystalline size of HAP nanoparticles are calculated by Debye Scherrer equation (Eqn.1), where $t_{(hkl)}$ is the mean size of crystalline domain, B is the line broadening at half maximum intensity, and $\theta_{(hkl)}$ is the Bragg angle [24]. In a study, the crystal size of nano HAP powders was calculated as 305 nm by Debye-Scherrer equation [23].

$$t_{(hkl)} = 0.9\lambda / B \cos\theta_{(hkl)} \quad (1.1)$$

The scan scale and scan speed should be adjusted as 3-100˚ for the 2θ angle range and 2^{o} per minute during working, respectively. By comparing the similarity of the peaks of the synthesized hydroxyapatite powder with natural hydroxyapatite, the success of the synthesis is evaluated [24]. In Figure 1.6, there is an example of XRD spectra that compares synthesized HAP nanoparticles with the one in the library [24].

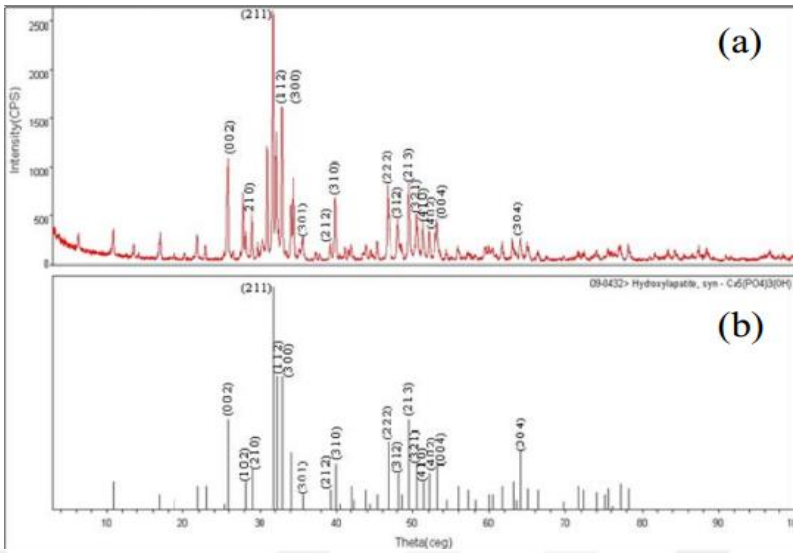

Figure 1.5a. XRD of HAP-A nanoparticles Figure 1.5b. XRD of library standard of hydroxyapatite [24]

To observe the functional groups of hydroxyapatite, FTIR analysis is commonly used. The groups of synthesized hydroxyapatite are detected as evident peaks corresponding to constant groups such as carbonate ions CO_3^{2-}, phosphate groups PO_4^{3-}, hydroxyl group OH^- and adsorbed water [26]. The wavenumbers (cm^{-1}) corresponding to the stretching vibrations of these functional groups at the synthesized hydroxyapatite particles are determined and compared with the standard wavenumber values of hydroxyapatite.

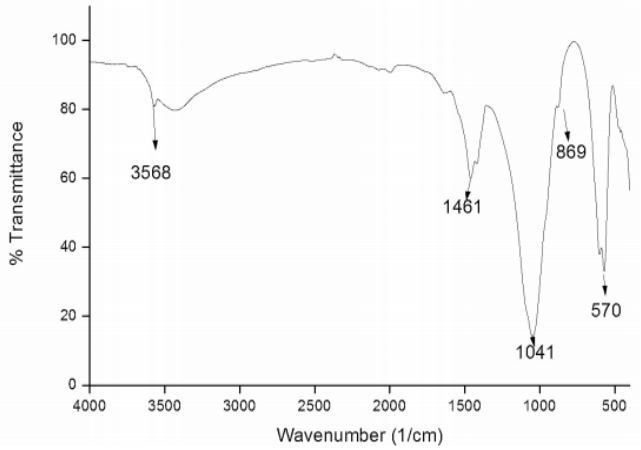

Figure 1.6. FTIR spectrum of nano-hydroxyapatite [26]

The FTIR characterization is acquired for almost all studies to investigate the functional groups of synthesized hydroxyapatite. In a recent study by Chandrasekar et al [27], the wet chemical technique were used to obtain nano-hydroxyapatite with stretching vibrations at peaks including stretching modes at range of 4000-500 cm^{-1} as shown in Figure 1.6 and Table 1.4.

Table 1.4. The functional groups of HAP nanoparticles [27]

Wavenumber cm^{-1}	Stretching mode	Functional group
3568	Ion stretching	OH^-
1461	Asymmetric stretching	CO_3^{2-}
1041	Asymmetric stretching	PO_4^{3-}
869	Out of plane bending mode	CO_3^{2-}
570	Asymmetric bending vibration	PO_4^{3-}

Parameters that affect the FTIR spectra are thermal treatment, lattice parameters, thermal stability, physical and chemical changes in morphology. HAP can be used as a biomaterial in the ceramic form by sintering its powder with heat treatment at high temperatures such as 1000-1350^{0}C for surface coating [28].

Differential Thermal Analysis and Simultaneous Thermogravimetric (DTA/TG) methods allow to analyze with respect to mass and thermal differences. TG analysis is a quantitative method which shows the responses to changes in mass. On the other hand, DTA method determines heat capacity or enthalpy changes in the reactions. These two most common techniques were combined first in 1955 by Paulik brothers [36]. The DTA/TG method is commonly used to observe the endothermal and exothermal regions and also to detect the weight loss and weight gain [37]. According to the DTA/TG curves, the hydroxyapatite thermal stability is determined and quantitative results can be obtained at various temperature ranges. Additionally, the main equation used in DTA/TG analysis is given as follows: [38]

$$Ca_{10}(PO_4)_6(OH)_2 \rightarrow Ca_{10}(PO_4)_6(OH)_{2-2x}O_x + xH_2O \quad (1.2)$$

The common chemical groups that correspond to absorption bands in FTIR are given in Table 1.5.

Table 1.5. FTIR absorption bands and chemical groups of synthesized HAP [28]

Chemical groups	**Absorption bands (cm^{-1})**	**Description**
CO_3^{2-}	873; 1450; 1640 [29];1650 [31]; 870 and 880; 1460 and 1530 [30]	Substitutes phosphate ion, B-type HAP is formed [29]
OH^-	3500 [29]; 630 and 3540 [31], [32]; 3570 and 3420 [35]; 1650 [31]	OH- ions show presence of HAP
Adsorbed water	2600 – 3600 [29]	Absorption bands become tighter by thermal treatment
HPO_4^{2-}	875 [31], [32]; 880 [33]	Refers to non-stoichiometric HAP [33]
PO_4^{3-}	460 [31], [32]; 560 - 600 [31], [32], [33] ; 602 -555 [35]; 960 [31], [32]; 1020 - 1120 [31], [32]; 1040 [35] 1000 - 1100 [34]	v2 [32] ; v4 [32] bending mode [35] ; v1 [32]; v3 [32] bending mode [35]
NO_3^-	820 and 1380 [31], [32]	Synthesis grounds vanishes during the calcification [32]

In a study by Agrawal et al [38], the hydroxyapatite powder was obtained by Sol-Gel method for biomedical applications. According to the DTA and TG analysis curves, the weight loss was observed as approximately %12 when the temperature was up to 220 ^{0}C and 40% weight loss was detected between 220^{0}C and 350^{0}C. At the 600^{0}C, the major

weight loss of hydroxyapaptite was obtained but when the temperature was up to 1200^{0}C there was no weight loss observed as shown in Figure 1.7 [38].

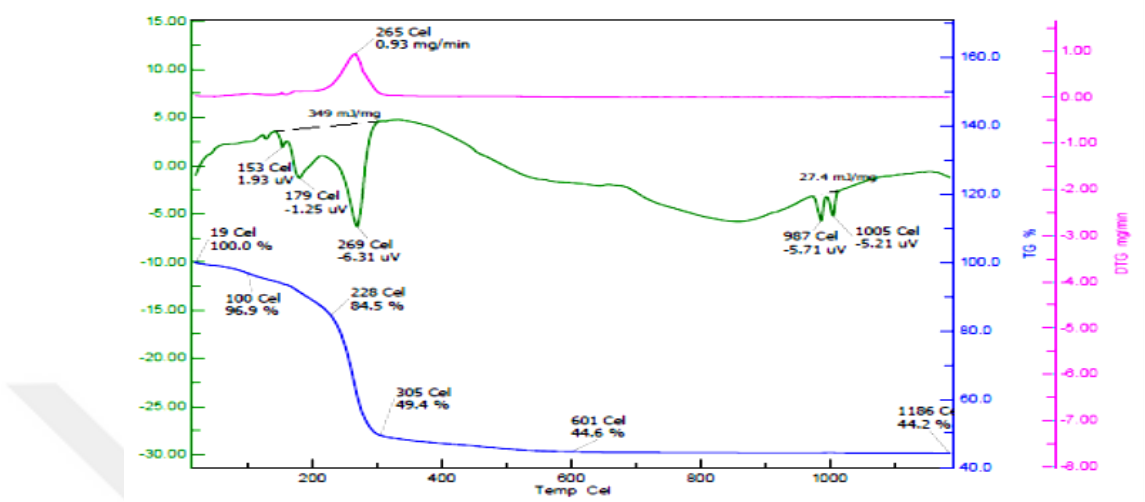

Figure 1.7. DTA/TG curves of sintered hydroxyapatite powder [38]

In the Figure 1.7, the blue line represents the percent weight loss of HAP via TG. The pink line shows the rate of weight loss in mg/min via DTA. The green line shows the UV absorption spectra values.

Transmission Electron Microscopy (TEM) and Scanning Eletron Microscopy (SEM) are often used to observe the morphologies of hydroxyapatite particles and to determine the diameters of particles in nanometer or micrometer scale. In a study by Agrawal [39], the nano-structured hydroxyapatite was synthesized in organic solvents and according to the TEM results, they found sub-micron to nano size- range particles with particle shapes such as rod-like crystals, spherical crystals and so on. According to the TEM micrographs given in Fig. 1.9, the shapes and dimensions of the nano-HAP powders are as follows: (a) rod-like crystal with 7 nm thickness / 66 nm length, and (b) a rod-like crystal with 6 nm thickness / 75 nm length.

SEM analysis also demostrates the morphology of hydroxyapatite particles and the size of particles in nano or micro scales. For example, the SEM micrograph (Figure 1.10) shows the agglomerated nanoparticles with sizes no more than 100 nm [40].

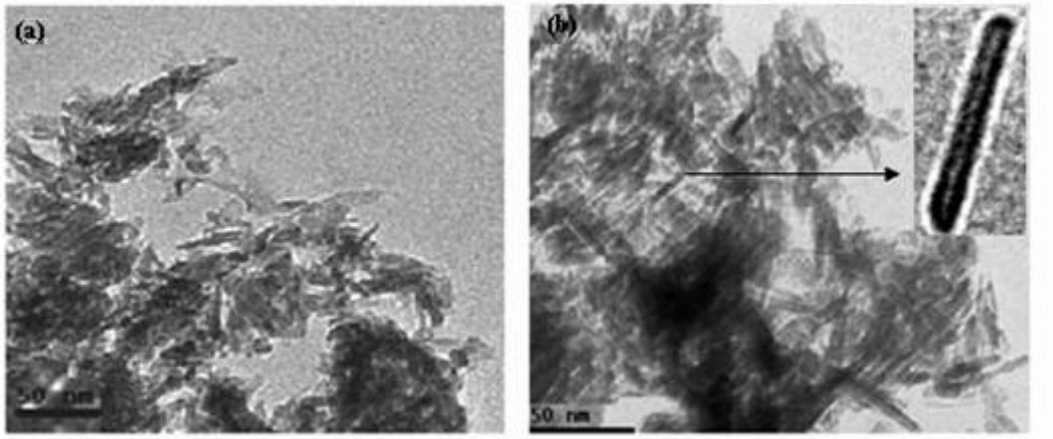

Figure 1.8a. TEM micrograph of nano-HAP powders at room temperature prepared in ethanol with slow addition mode, Figure 1.8b. TEM micrograph of nano-HAP powders at room temperature prepared in ethanol with rapid mode [39]

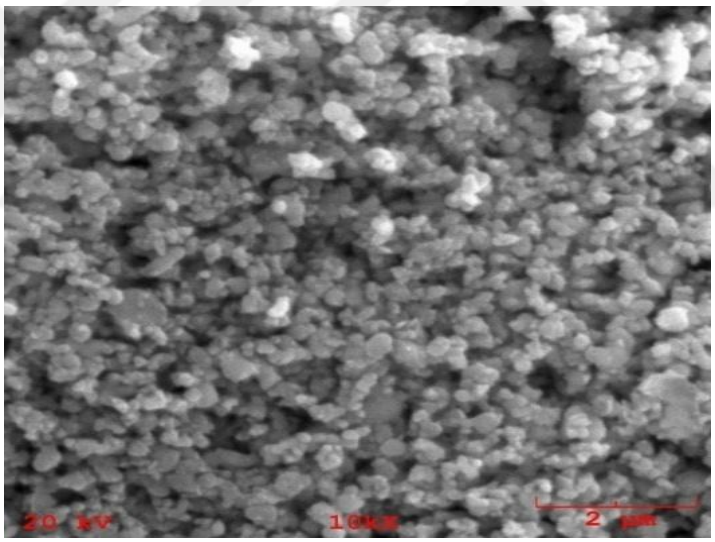

Figure 1.9. SEM micrograph of hydroxyapatite powder [40]

1.3. Bone Graft Substitutes for Bone Regeneration

Even before B.C., replacement of missing bones and teeth with other materials has been a need for people. For example, archeological studies have proved the replacement of human teeth with several different materials ranging from corals to metals such as gold or silver [5].

There are mainly two kinds of bone tissue replacements; endogenous and exogenous. Both implementations have certain disadvantages. Since endogenous bone substance comes with additional surgeries, the possibility of rejection by the human body is very high. As a result, artificial hard tissue replacement outshines endogenous or exogenous bone replacements for been as a nature bone [5].

The mimicking of micro- and macroporous architecture of inorganic phase of living bone is the main purpose of bone replacement [5]. The biological mechanism of living bone grafting consists of severals steps such as osteoconduction, osteoinduction and osteogenesis.

(i) Osteoconduction: Osteoconduction means that bones can grow on a surface or within the pores of a surface [2].

(ii) Osteoinduction: Just before the beginning of new bone formation, osteoinduction occurs, which is essential for the differentiation of osteogenitor cells to osteoblasts. The osteoblasts speed up the integration of the graft. The most popular type of osteoinductive cell mediators are bone morphogenetic proteins (BPMs) [2].

(iii) Osteogenesis: In the osteogenesis, vital osteoblasts originate from the bone graft material, and they lead the growth of new bone [2].

Artificial approaches for bone replacement have different types such as autografts, autologous bone grafts, allografts, synthetic variants, xenografts, alloplastic grafts [2].

- Autografts (Autogenous): In this method, the graft belongs to the patient's own body. Therefore, the rejection risk is very low and this method is the most preferred. The disadvantage is the need of an additional surgery [2].

- Allografts: The allograft method is similar to the autogenous but this time the needed bone is derived from another donor. Even though grafts in larger sizes can be

supplied by this method, the risk of pathogen transmission and rejection is very high [2].

- Xenografts: The needed bone is supplied from species other than humans, such as cows and baboon. Xenografts are exposed to greater risks of infection [2].

- Synthetic variants: Ceramics such as calcium phosphates, calcium sulphate, and bioglass can be used as artificial bone since they are bioactive materials. This method resembles autogeneous bone grafting but this time the rejection and infection risks are much less [2]. Natural polymers (such as collagen) can be also used as artificial bone. However, their structure is very limited. Therefore, synthetic polymers are more popular than the natural ones despite their biocompatibility problems [2]. Hydroxyapatite is another synthetic bone graft. Thanks to its osteoconduction, hardness and acceptability by bone, hydroxyapatite is the most used one as a bone grafting technique [2].

- Alloplastic grafts: Calcium hydroxide coated polymers are used in this method. The infection risk is very low and the mechanical properties are better [2].

1.4. Hydroxyapatite-Polymer Composite Materials

Bone is a natural complex structure which contains a high density of cortical bone and a low density of trabecular bone. This complexity of bone provides the hierarchical structure and some of its components such as extracellular matrix, collagen fibrils, apatite crystals etc. make the bone for hard scaffold structures [42]. These properties of bone should be considered while designing biomimetic bone graft-materials. Properties such as biocompatibility, biodegradability, bioactiveness are essential in the design of biomaterials which are similar to natural bone. Additionally, osteoconductivity, osteoinductivity, apatite crystallization should be considered [25].

Various synthetic or natural polymers are used as composite materials with calcium phosphate. In recent years, hydroxyapatite-polymer composites have been used for similar

mechanical properties to the natural bone. Moreover, the surface modification of hydroxyapatite particles enables the properties of bone to be improved [4].

Hydroxyapatite-polymer composite materials are more suitable composite materials than pure hydroxyapatite materials. Furthermore, hydroxyapatite strengthens the polymer stiffness and bonding properties of the bone [42]. On the other hand, pure hydroxyapatite is not strong enough for high load-bearing applications due to its fragility, low mechanical strength, and weak fatigue resistance. To overcome these problems and to design a material similar to the nature bone, composites of hydroxyapatite with polymers are explored [43].

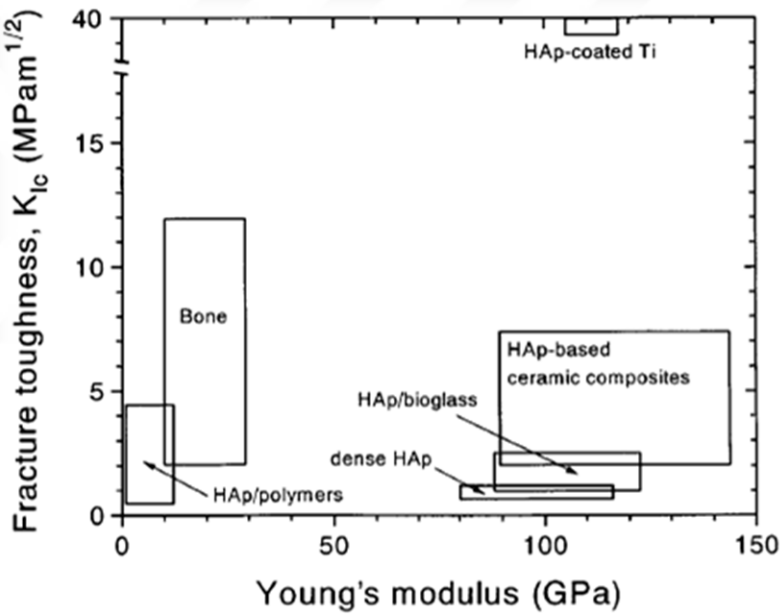

Figure 1.10. Relationship between fracture toughness and Young's modulus of the current biomaterials for bone tissue replacements [16]

1.4.1. Hyaluronic acid-Hydroxyapatite Composite Materials

Hydroxyapatite is most useful in bone replacement when used as composites with materials such as gelatin, collagen, and polyamide. Also, nanocomposite materials are formed with silk fibroin and hyaluronic acid [44].

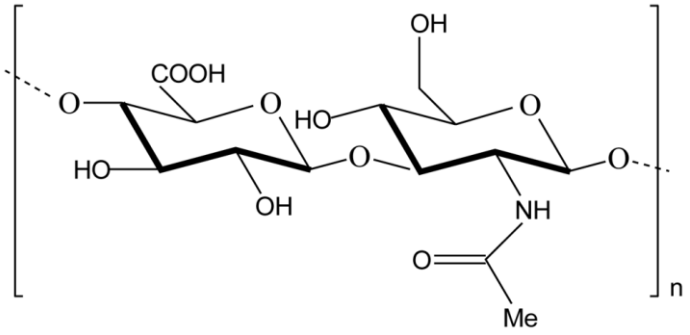

Figure 1.11. The chemical structure of hyaluronic acid

Hyaluronan is a negatively charged hydrophilic biopolymer, which allows the composites to function under aqueous conditions [46].

Hyaluronic acid (hyaluronan) is one of the glycosaminoglycans and is found in cartilage. It serves as a resisting compressive force in the joints and tissues. Hyaluronic acid is synthesized in the basal side of the epithelium, which is present in the cornea and heart.

Hyaluronic acid is capable of improved cohesion for composite materials so it would be advantageous to use hyaluronic acid with hydroxyapatite nanoparticles. Furthermore, the surface activity is one of the most important properties of materials for bone growth. Thus, hyaluronic acid plays a key role as a component of composite materials while designing highly bioactive scaffolds [46].

1.4.2. Surface Modification of Hydroxyapatite

The surface of hydroxyapatite is directly in contact with the environment. The functional groups, surface change, and acid-base balance are important factors for hydroxyapatite surfaces. These surface properties, however, can change when HAP interacts with other materials to form composites [4].

There are many reasons to tailor the surface of hydroxyapatite nanoparticles such as preventing the hydroxyapatite nanoparticles to aggregate. Adhesion reactions are also studied to control the affinity of modified HAP surface with other chemicals [47,48].

The hydrophilic groups of hydroxyapatite are the P-OH groups and exist on the surface. They represent adsorption sites for other molecules and react with many organic/ inorganic substances while producing composites. Moreover, they provide a preferable environment for protein adsorption and a better dispersibility in the aqueous phase. The number of P-OH groups is important for adsorption. It is also possible to make these hydrophilic groups hydrophobic by modifying the surface with alkyl groups [48].

The other active groups of hydroxyapatite surfaces are hydroxyl groups. But the modified-surface hydroxyl groups are not preferable because of their limited bioactivity [48].

There are many methods to modify the surface properties of hydroxyapatite by the use of silane coupling agents, organic isocyanates, zirconyl salts, and polyacids [48].

Organic molecules or polymers give an increased chance to control the surface properties of HAP. There are two methods of modification with organic molecules. 1) Surface adsorption. 2) Grafting organic molecules to the surface of hydroxyapatite with a covalent bond to the hydroxyl groups [48].

1.4.3. Polymer Adsorption on Hydroxyapatite

Many kinds of polymers can be adsorbed onto the surface of hydroxyapatite. Hydrogen bonding plays a key role for surface adsorption. The OH groups serve as water binding sites. The successful chemical bonding between polymer matrix and the hydroxyapatite nanoparticles, substantially improves the mechanical properties of composites. Thus, there has been lots of studies on adsorption of different proteins such as enzymes and anionic macromolecules such as polyacrylic acid on hydroxyapatite [49].

1.4.4. Adsorption of Catechol on Hydroxyapatite

The surface charge of hydroxyapatite is positive and anions such as carboxymethylcellulose or polyacrylic acid are preferably adsorbed at pH between 6.5 and

8.5. Rather than the electrostatic forces between hydroxyapatite and the partially ionized polymers, the hydrogen bonding is more important [5].

In these adsorption processes, by the help of the mussels` capability to form powerful adhesive bonds to the substrates in wet states, natural adhesives derived from mussels have received substantial recent attention [49].

Mussels contain high levels of 3,4-dihydroxy-L-phenylalanine (DOPA, an amino acid characterized by its catechol (3,4-dihydroxyphenyl) group and lysine amino acids. The catechol group carries an adhesive property, has a strong affinity to hydrophilic polymers and a large capacity for hydrogen bonding [49].

In a study by Lee et al [50], the difference of catechol and catechol containing chemicals with various other simple chemical groups are compared with respect to work of adhesion and binding constants (Fig. 1.13 and Table 1.6). 3-Hydroxytyramine and gallotannic acid have a catechol group containing an amine group. Hexanoic acid, hexylamine, and hexanol involve carboxylic acid, amine, and alcohol groups, respectively [51]. Tannic acid, catechol, 3-hydroxytyramine and pyrogallol show similar adhesion affinity [51].

Table 1.6. Catechol and catechol containing chemicals [50]

	Work of Adhesion (MJ/m2)	**K (ml/mol)**
Tannic acid	91.33 ± 3.20	1.86E+09
Catechol	88.23 ± 2.93	3.31E+07
Hydroxytyramine	90.05 ± 3.79	2.23E+07
Hexanoic acid	68.19 ± 5.95	1.73E+07
Pyrogallol	90.35 ± 3.34	4.08E+06
Hexylamine	57.05 ± 3.19	3.83E+06

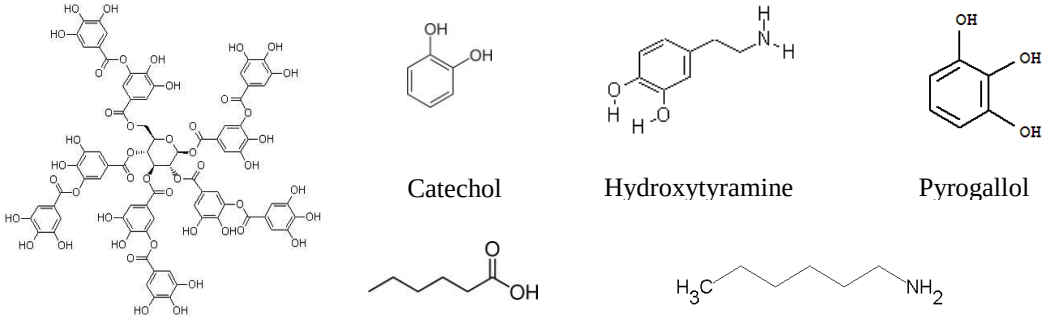

Figure 1.12. The chemical structure of catechol and catechol containing chemical groups

2. OBJECTIVES AND METHODOLOGY OF THE PROJECT

Our goal was to modify hydroxyapatite nanoparticles (HAP) with a biopolyelectrolyte, hyaluronic acid (HYA), to form a nanocomposite which mimicks bone. For this purpose, hydroxyapatite was prepared (1) in the presence of 2-carboxyethyl phosphonic acid, (2) by applying citrate treatment, (3) by controlling the nucleation time following the methods in the literature.

Physical adsorption and chemical conjugation techniques are commonly used to modify hydroxyapatite. In this work, polyacrylic acid (PAA) was bound via physical adsorption onto suspensions of hydroxyapatite nanoparticles. The modification degree of hydroxyapatite with PAA was compared with unfunctionalized and catechol-functionalized hyaluronic acid (HYA). To prove the modification of hydroxyapatite, characterization analysis were used such as FTIR, TGA and SEM and outcomes were discussed.

3. EXPERIMENTAL

3.1. Materials and Methods

All reagents were purchased from commercial sources (Merck, Sigma Aldrich and VWR) and were used without any further purification. Dry solvents were prepared by drying over molecular sieves. Hyaluronic acid sodium salt was obtained from Lifecore Biomedical (Chaska, MN, USA) while commercial hydroxyapatite was purchased from Sigma-Aldrich.

Particle characterizations involved Fourier transform infrared (FTIR) spectroscopy (Perkin Elmer 1600 Series), Dynamic Light Scattering (Brookhaven 90 Plus Particle Size Analyzer), Powder X-Ray Diffraction (Rigaku D/max-2200/PC), Scanning Electron Microscope (Phillips XL30). The weight % of hydroxyapatite modification was estimated by thermogravimetric analysis (TGA Q50 Universal Analysis 2000). Type 1 and Type 2 titrations were done with a colorimeter (Brinkmann Probe Colorimeter PC 950).

3.2. Synthesis of Calcium Phosphate Nanoparticles

3.2.1. Method 1: Synthesis of calcium phosphate (CP) nanoparticles containing 2-carboxyethylphosphonic acid (CEPA) [51]

This method is adapted from the article of Kotov and his coworkers [51]. Here, the aim was to control the size of the hydroxyapatite nanoparticles and prevent them from aggregation by incorporating 2-carboxyethyl phosphonic acid (CEPA) as a stabilizing agent. Furthermore, it is assumed that the presence of phosphorus in CEPA would favor its absorption with the body [51]. The stoichiometry of the reaction mechanism is as follows:

$$Ca(NO_3)_2 + 6\ H_3PO_4 + 20\ NH_4OH \rightarrow Ca_{10}(PO_4)_6(OH)_2 + 18\ H_2O + 20\ NH_4NO_3 \quad (3.1)$$

The calcium solution was a mixture of 0.15 mmol (0.0356g) calcium nitrate tetrahydrate (>99.0%, Lot# MKBF0637V, Product# C1396-500G,Sigma-Aldrich) and 0.30 mmol (0.0461g) of CEPA (2-carboxyethylphosphonic acid) (94%, Lot# 03721EJ, Product# 22,855-9-5G,Aldrich), which were dissolved in Milli-Q water, and the final volume was set to 10 ml. The pH of this solution which was 1.88 at the beginning of mixing two materials increased to 6.83 after adding ammonium hyroxide (28-30%, Lot# K40199523 922, Product# 1.05423.2500, Merck) in 10 minutes. Then, an additional amount of 0.52 mmol (0.0801g) of CEPA was added to the 0.4 ml of the above solution under stirring. At this stage, the pH was read as 1.72.

The phosphate solution was prepared by diluting 0.0776 ml of 0.98 M (0.9610 g was dissolved in 10 ml milli-Q water) phosphoric acid (>99.999%, Lot# MKBD0582, Product# 466123-25G,Aldrich) with Milli-Q water until the final volume was 10 ml. The pH of the phosphate solution was then adjusted from 2.32 to 9.32 by adding ammonium hydroxide.

In the last step, the phosphate solution was added to the Ca/CEPA solution at room temperature while stirring. At this time, the pH of mixed solution was 2.45 and increased to 9.62 by addition of ammonium hydroxide in 10 minutes.

During the first 25 minutes, the pH decreased to 9.50 since the beaker was not closed with any lid (due to presence of CO_2 in air).

Rinsing the dispersion with ethanol (Absolut, Lot# 92010, Product# 32221-2.5L, Sigma-Aldrich) allowed the CP NPs to precipitate out of the solution. The particle dispersion was diluted in 4:1 ratio with ethanol in two different centrifuge tubes and centrifuged with a Universal 320 Hettich Zentrifugen at 6000 rpm for 20 min which resulted in two layers. Then the supernatant was decanted and the particles were washed again as above. After the second centrifugation, there was a colloidal suspension at the bottom of the tube. After the supernatant was decanted, only a small amount of ethanol stayed behind. Then, we added less than 1 ml of milli-Q water to the particles. All this washing process was followed for both of the samples in the two centrifuge tubes and they were kept at the room temperature for overnight.

The next day, the sample in one of the centrifuge tubes was transfered into the other one by washing several times with Milli-Q water of 20 ml. Following freezing the fluffy colloidal suspension at -80^{o}C for 80 min, it was put into the lyophilizer.

During the lyophilization, one of the frozen tubes was closed with a lid that had syringe needle inserted in while the other one was closed with a paper towel. Unfortunately, lyophilization was not achieved with the tube with a syringe needle on the lid. The other one was put in a vacuum oven for 24 hours in order to have a fully dried sample. The weight of the product was $1.1x10^{-3}$ g with a yield of 1 % by wt.

As the weight of obtained sample was very low to do any further experiment, the volume of calcium and phosphate solutions using in the experiment was increased by three times in one trial and then ten times in another trial but with no change in molarities of both of the solutions.

It is known that temperature and the amount of stabilizing agent, which is CEPA in this method, are effective parameters to control the diameter of the obtained nanoparticles. It is expected that the diameter of the particles would be less at low temperature or when higher amounts of stabilizing agent are used. Therefore, preparation of calcium phosphate nanoparticles was repeated (1) by using extra amount of CEPA, (2) in the absence of CEPA, and (3) at 0 ^{o}C in order to find out the differences in the diameter of obtained particles.

3.2.2. Method 2: Synthesis of calcium phosphate nanoparticles in the presence of citrate [52]

Since the yields of Method 1 were still low, we tried another method of hydroxyapatite preparation [52]. In this new method, citric acid was used as the stabilizing agent that would prevent hydroxyapatite aggregation. The yield of the reaction below was 30% by weight and the particles turned out to be as large as micron-size.

Flow chart of the method and stoichiometry of the reaction are given below:

$$10Ca(NO_3)_2.4H_2O+6(NH_4)_2HPO_4+8NH_4OH \rightarrow Ca_{10}(PO_4)_6(OH)_2+20NH_4NO_3+46H_2O \quad (3.2)$$

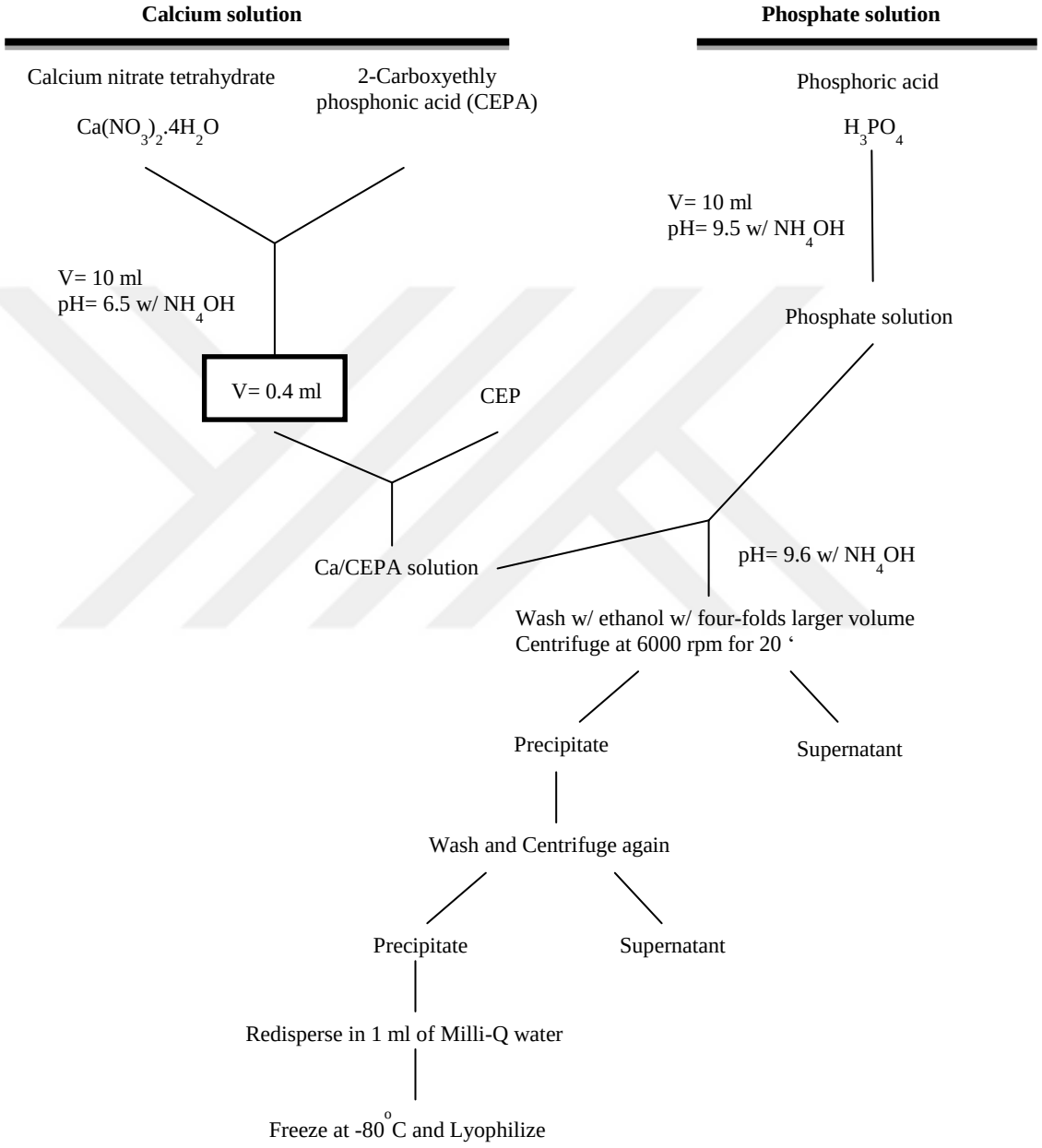

Figure 3.1. Preparation method for hydroxyapatite nanoparticles with Kotov’s method

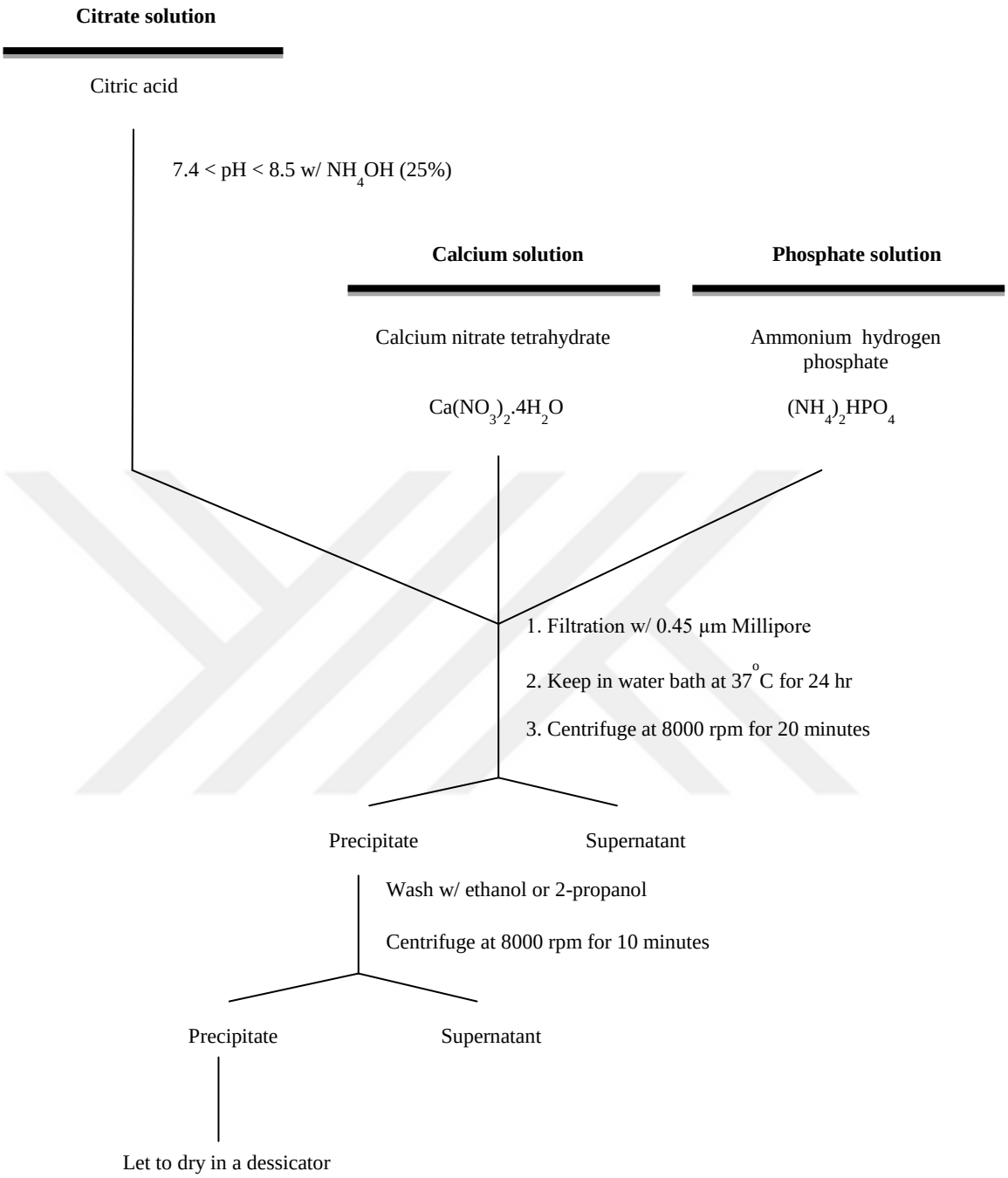

Figure 3.2. Preparation method for hydroxyapatite nanoparticles with Costa's method

0.6 M citric acid monohydrate ($C_6H_8O_7.H_2O$) solution was prepared in Milli-Q water and the pH of the solution was adjusted to 8.6 with ammonia. 100 ml of 0.2 M Calcium nitrate tetrahydrate ($Ca(NO_3)_2.4H_2O$) and 100 ml of 0.2 M Diammoniumbiphosphate ($(NH4)_2HPO_4$) solutions were mixed with 100 ml of above $C_6H_8O_7.H_2O$ solution at RT (21^oC). Then the pH of the final mixed solution was brought to

9.5 with ammonia, and immediately filtered with a 3 μm of filter paper (NitroCellulose, Millipore). In the original method, the solutions were mixed and filtered with a 0.45 μm of filter paper, then kept in a water bath at 37 ^{o}C for 24h. As it might be a driving force for aggregation, the pH of the mixed solution was adjusted to 9.5 before filtering differently from the normal procedure.

After centrifugation at 6000 rpm for 25 min, the precipitate was washed with 20 ml of 2-propanol and again centrifuged at 6000 rpm for 20 min. The supernatant was disposed and the precipitate with a minimal amount of 2-propanol was dried in the vacuum dessicator for 12 h.

Method 2 was repeated with the exception that the pH of the final mixed solution was not adjusted. After the first centrifugation step, however, no precipitation was observed. Instead, it was all clear solution.

3.2.3. Method 3: Synthesis of calcium phosphate nanoparticles with adjustable crystallinity [53]

This method by Epple and coworkers [53] was also tried since we were not successful at the previous methods to obtain monodisperse nanoparticles with diameters less than 100 nm. The advantage of Epple's method is the control of the nucleation time by a vacuum pump, controlled aggregation by immediate filtering and washing with isopropanol, and controlled nanocrystallinity according to the selected drying method. The yield during our trials was around 85 % by weight. The flowchart of this method is given in Figure 3.3 while the reaction stoichiometry is given below:

$$10Ca(NO_3)_2+6(NH_4)_2HPO_4+8KOH \rightarrow Ca_{10}(PO_4)_6(OH)_2+12NH_4NO_3+8KNO_3+6H_2O \quad (3.3)$$

In this method, 6.75 mM of $Ca(NO_3)_2$ and 4.05 mM of $(NH_4)_2HPO_4$ reagents were prepared in Milli-Q water and the pH of both solutions was adjusted to 10 with 1 M KOH before mixing them together. The solutions of calcium and phosphate, which were initially prepared in an ice bath to bring the temperature to 4^{o}C, were continuously added together.

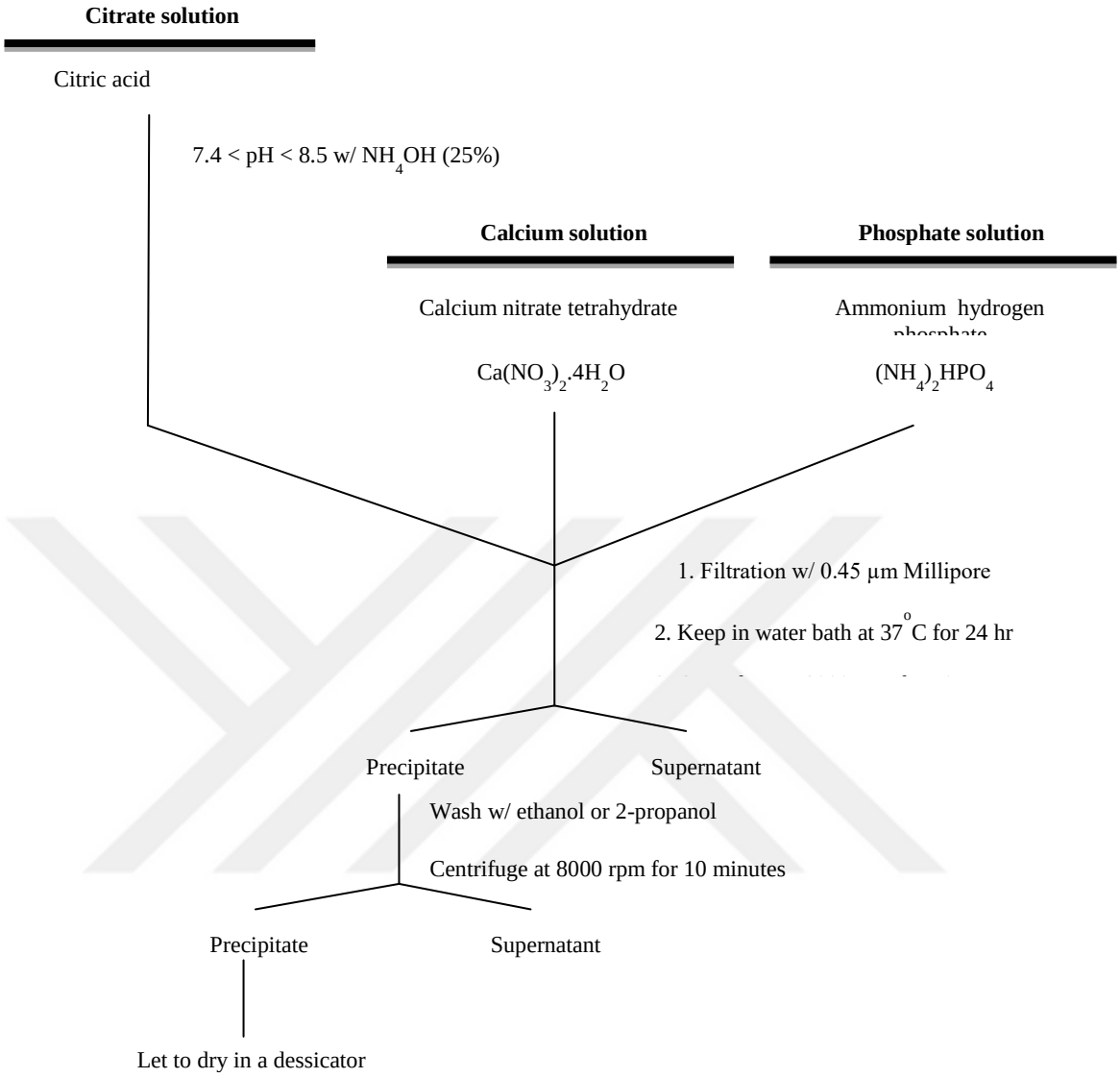

Figure 3.3. Preparation method adapted from Epple and his co-workers

The pump drive used for mixing the solutions was adjusted to 12.5 rpm which allowed the flow of about 30 ml of solutions in a minute. Then the mixture was immediately poured onto a filter. This last step enabled the precipitates to remain nanocrystalline. The precipitate on the filter paper was washed with 50 ml of 2-propanol and let to dry in air (26.47 ml/min). This whole method (pump drive: 27.97 ml/min) was repeated again by changing the drying method; where the washed precipitate was taken to a centrifuge tube, dissolved in 7.5 ml of Milli-Q wate, and then frezee-dried. And the yield was around 85 % by weight.

3.3. Polyelectrolyte Adsorption onto Hydroxyapatite Nanoparticles

3.3.1. Control Experiment 1: Adsorption of polyacrylic acid (PAA) onto hydroxyapatite nanoparticles

0.25 or 0.5 mg/ml of PAA and 1 mg/ml of hydroxapatite (Sigma Aldrich) solutions were prepared in ethanol and stirred for 3 h. Previoulsy prepared hydroxyapatite solutions were not used for these experiments since we could only get monodisperse spherical nanoparticles bigger than the commercial samples obtained from Sigma-Aldrich.

50 ml of each of the PAA and hydroxyapatite solutions were mixed with a residence time of 420 sec; i.e. the mixture was stirred for 420 s. Then the mixture was loaded into four centrifuge tubes and centrifuged at 6000 rpm for 20 min. The supernatant was decanted and the precipitates were washed with 25 ml of ethanol and centrifuged at 6000 rpm for 30 min again. Then, the supernatant was decanted while the precipitate was dried in a vacuum dessicator for 48 h.

3.3.2. Control experiment 2: Adsorption of unfunctionalized hyaluronic acid onto hydroxyapatite nanoparticles

1 mg/ml hydroxyapatite solution was prepared in Milli-Q water. The pH of the hydroxyapatite solution was adjusted from 9.98 to 5.98 after stirr for 2 h.

0.25 mg/ml unmodified hyaluronic acid (150 kDa) was prepared in Milli-Q water. After stirring the hyaluronic acid solution for 2 h, the pH was adjusted from 7.06 to 4.91. Then both solutions were mixed together with a residence time of 420 s. During this stirring, the pH of the mixed solution increased from 4.80 to 6.14 without any external adjustment of the pH. Then, the mixed solution was filtered with a 11 μm of filter paper before the supernatant was centrifuged at 6000 rpm for 30 min. The precipitate was dried in a vacuum dessicator for 12 h.

We repeated this experiment in another trial where the mixture was not filtered after 420 seconds of residence time.

3.3.3. Adsorption of Catechol Functionalized Hyaluronic Acid onto Hydroxyapatite Nanoparticles

In order to attach HYA onto HAP, the chosen methodology is adsorption of HYA through catechol functionalization of HYA`s carboxyl groups. The catechol modified HYA samples were prepared by Fatih [54]. Driving forces for HAP – Catechol adsorption are explained schematically in Figure 3.4.

The control experiment was also done with unfunctionalized hyaluronic acid. Polyelectrolyte modified samples were analyzed with FTIR and TGA.

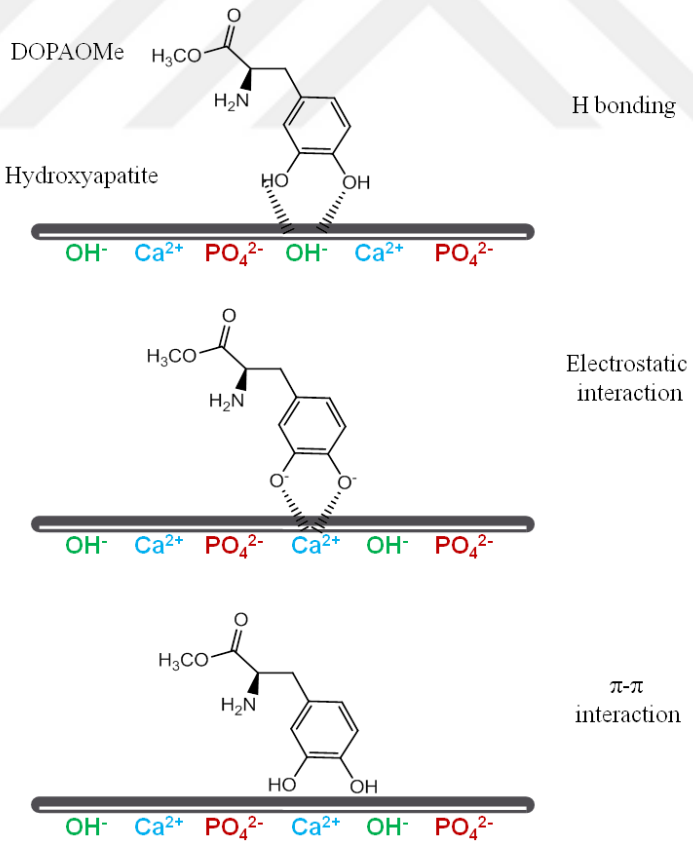

Figure 3.4. Driving forces for HAP – Catechol adsorption

Preparation method of modified hydroxyapatite nanoparticles was summarized in Table 3.1.

Table 3.1. Summary of experiments with unfunctionalized hyaluronic acid adsorption onto hydroxyapatite nanoparticles

Concentration of HAP	**Concentration of HYA**	**Preparation Conditions**
1 mg/ml – HAP from SIAL	1 mg/ml – 150 kDa of unfunc. HYA	*pH of HAP : 10.10→6.09 *pH of HYA : 7.06→5.57 *Stir both solutions for 3 h *pH of the mixed solution (50 ml of each) : 6.21→6.13 *420 sec as a residence time for the mixed solution *Centrifuge at 6000 rpm, 30 min. *Dry in a vacuum dessicator for 12h
1 mg/ml – HAP from SIAL	1 mg/ml – 234 kDa of unfunc. HYA	*Stir both solutions for overnight *No pH arrangements separately *pH of the mixed solution (50 ml of each) : 9.66→5.89 *Separate the mixed solution in half **420 sec as a residence time for half (50 ml) of the mixed solution **12h as a residence time for half (50 ml) of the mixed solution *Centrifuge at 6000 rpm,30 min. *Dry in a vacuum dessicator for 12h
1 mg/ml – HAP from SIAL	0.50 mg/ml – 234 kDa of unfunc. HYA	*Stir both solutions for overnight *No pH arrangements separately *pH of the mixed solution (50 ml of each) : 9.50→5.90 *Separate the mixed solution in half **420 sec as a residence time for half (50 ml) of the mixed solution **12h as a residence time for half (50 ml) of the mixed solution *Centrifuge at 6000 rpm,30 min. *Dry in a vacuum dessicator for 12h

Our method for the adsorption of catechol-functionalized HYA onto HAP is summarized in Figure 3.5.

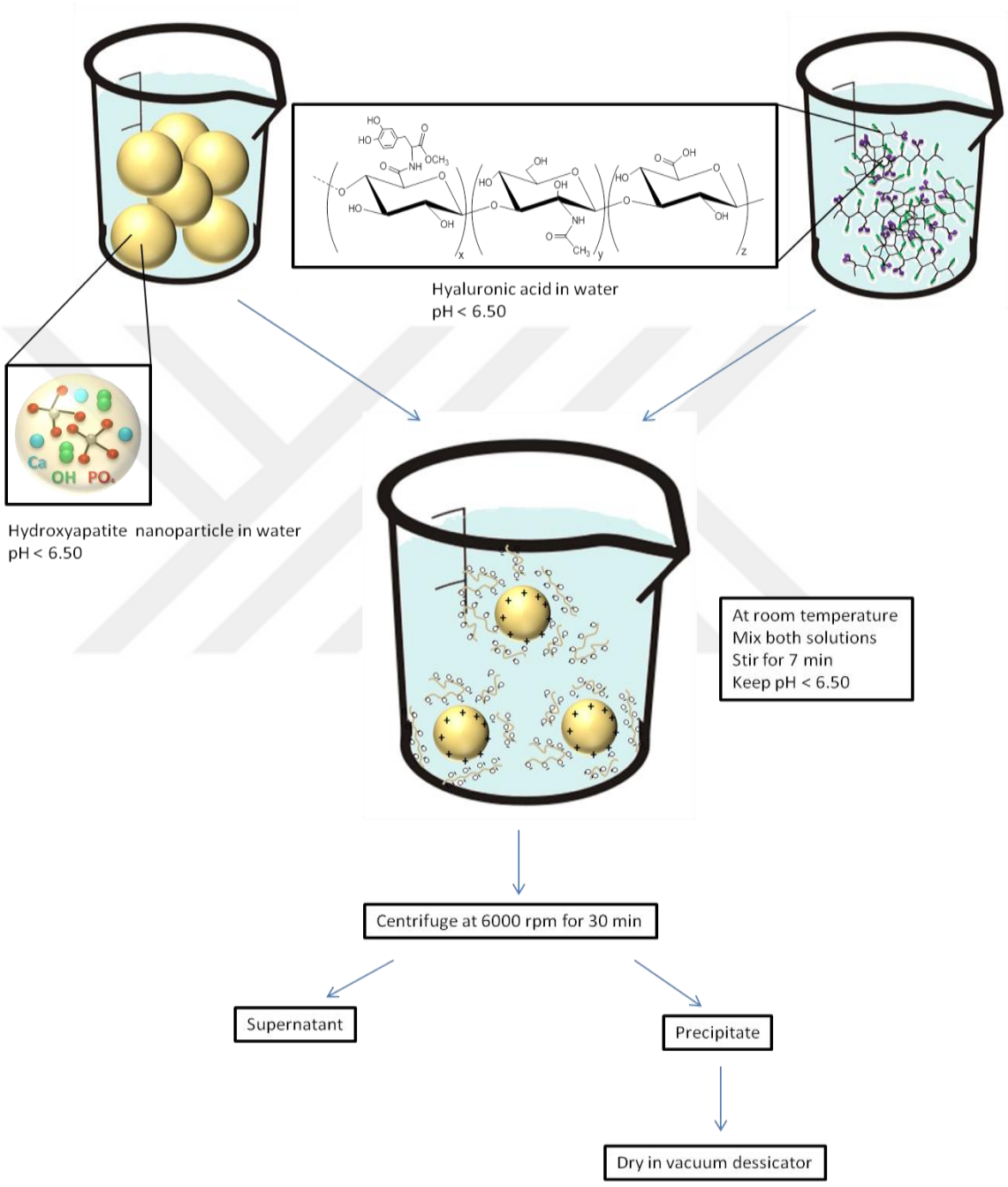

Figure 3.5. The schematic process of catechol functionalized hyaluronic acid adsorption onto hydroxyapatite nanoparticles

Table 3.2. Summary of experiments with hyaluronic acid adsorption onto hydroxyapatite nanoparticles

Concentration of HAP	**Concentration of HYA**	**Preparation Conditions**
1 mg/ml – HAP from SIAL	1 mg/ml – 150 kDa of unfunc. HYA	*pH of HAP : 10.10→6.09 *pH of HYA : 7.06→5.57 *Stir both solutions for 3 h *pH of the mixed solution (50 ml of HAP and 50 ml of HYA) : 6.21→6.13 *420 sec as a residence time for the mixed solution *Centrifuge at 6000 rpm, 30 min. *Dry in a vacuum dessicator for 12h
1 mg/ml – HAP from SIAL	1 mg/ml – 234 kDa of unfunc. HYA	*Stir both solutions for overnight *No pH arrangements separately *pH of the mixed solution (50 ml of HAP and 50 ml of HYA) : 9.66→5.89 *Separate the mixed solution in half *420 sec as a residence time *Centrifuge at 6000 rpm, 30 min. *Dry in a vacuum dessicator for 12h
1 mg/ml – HAP from SIAL	1 mg/ml – 150 kDa of Catechol func. HYA ($pH_{modification}$:7.0, Catechol modification: 4%, oxidation:5.7%)	*pH of HAP : 9.55→5.96 *pH of HYA : 3.76→6.36 *Stir both solutions for 3 h *pH of the mixed solution (50 ml of HAP and 50 ml of HYA) < 6.5 *420 sec as a residence time for the mixed solution *Centrifuge at 6000 rpm, 30 min. *Dry in a vacuum dessicator for 12h
1 mg/ml – HAP from SIAL	1 mg/ml – 234 kDa of Catechol func. HYA ($pH_{modification}$:7.45, Catechol modification: 4.29%, oxidation:45%)	*pH of HAP : 9.55→5.96 *pH of HYA : 3.71→6.65 *Stir both solutions for 3 h *pH of the mixed solution (50 ml of HAP and 50 ml of HYA) < 6.5 *420 sec as a residence time for the mixed solution *Centrifuge at 6000 rpm,30’ *Dry in a vacuum dessicator for 12h

3.4. Characterization

3.4.1. FTIR Characterization

FTIR spectra were taken with a Perkin Elmer 1600 FT-IR spectrometer using KBr discs.

3.4.2. TGA Characterization

TGA analyses were performed at TGA Q50 Universal Analysis 2000.

3.4.3. XRD Characterization

XRD analyses were performed at Rigaku D/max-2200/PC YD2798N for solid samples.

3.4.4. DLS Characterization

DLS analyses were performed at Brookhaven Instruments Corp. 90Plus Particle Sizing Software Ver. 3.95.

4. RESULTS AND DISCUSSION

4.1 FTIR characterization analysis results

4.1.1. FTIR results of calcium phosphate nanoparticles in the absence of 2-carboxyethylphosphonic acid (CEPA)

FTIR was done for calcium phosphate nanoparticles that do not contain CEPA. As shown in Fig 4.2, four other peaks were detected (1046, 876, 537, 415 cm^{-1}), which were attributed to PO_4^{-3} groups of HAP. Also, there is a peak around at 1440 cm^{-1} due to the C=O groups in air; i.e. in CO_2. The peak observed at 3219 cm^{-1} was because of NH_4^+ of NH_4NO_2 (ammonium nitrate).

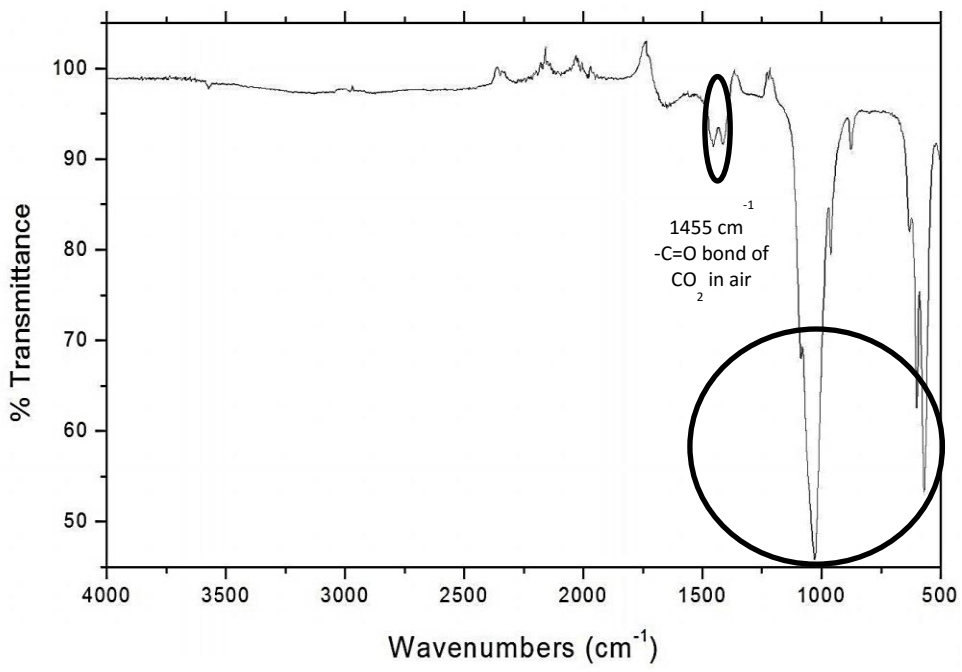

Figure 4.1. FTIR spectra of HAP (purchased from Sigma Aldrich (SIAL))

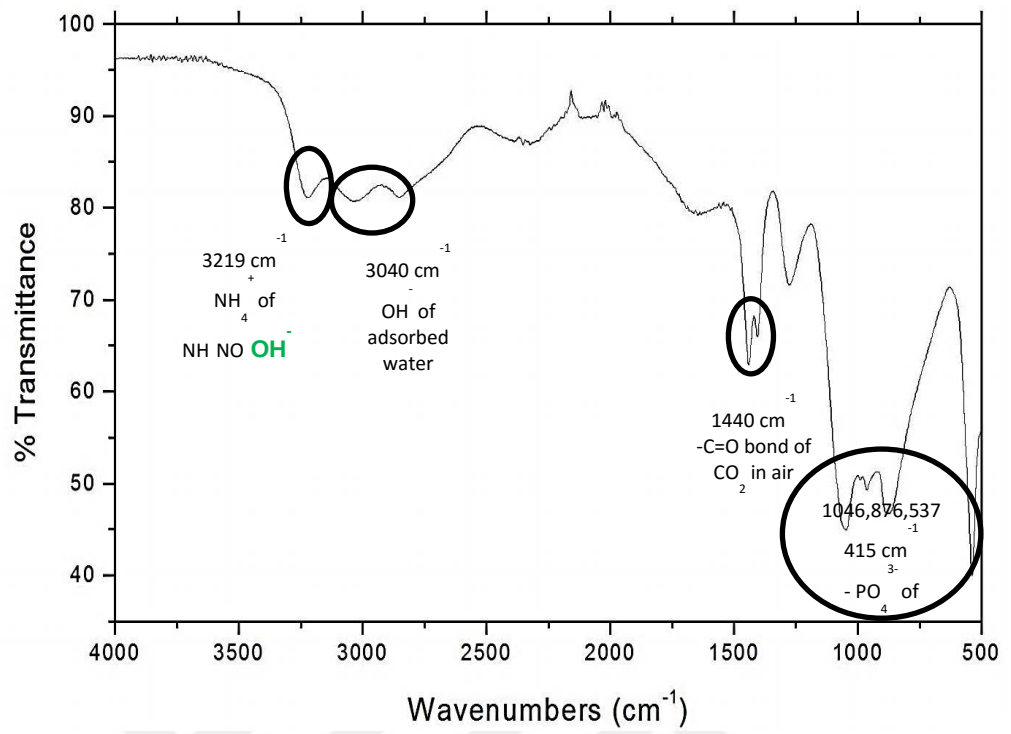

Figure 4.2. FTIR spectra of the HAP solid sample which was prepared without 2-carboxyethylphosphonic acid (CEPA) (Kotov's method)

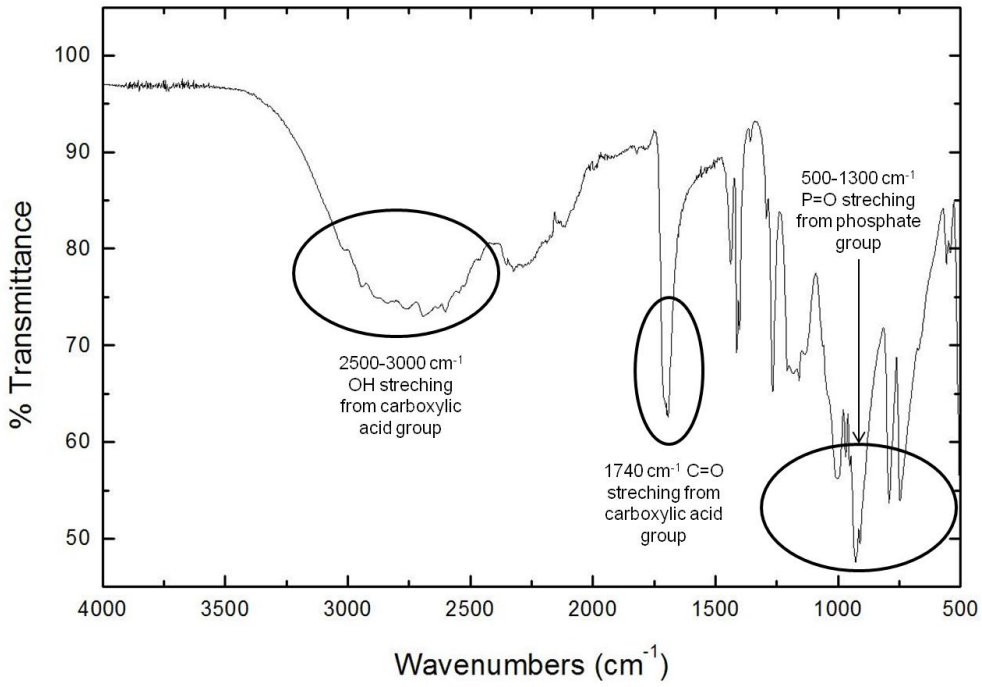

Figure 4.3. FTIR spectra of the pure CEPA (purchased from Sigma Aldrich)

4.1.2. FTIR results of calcium phosphate nanoparticles with treatment of citrate species

The calcium phosphate nanoparticles were synthesized with the treatment of citrate species. According to the FTIR graph (Figure 4.2) a peak was observed at 1573 cm^{-1} which demostrates the presence of $–COO^-$ bond of citrate specimens. Additionally, the same five peaks from 565 to 1020 cm^{-1} were due to PO_4^{-3} groups of HAP. And also a peak for OH- hydroxyl group was found at 3050 cm^{-1}.

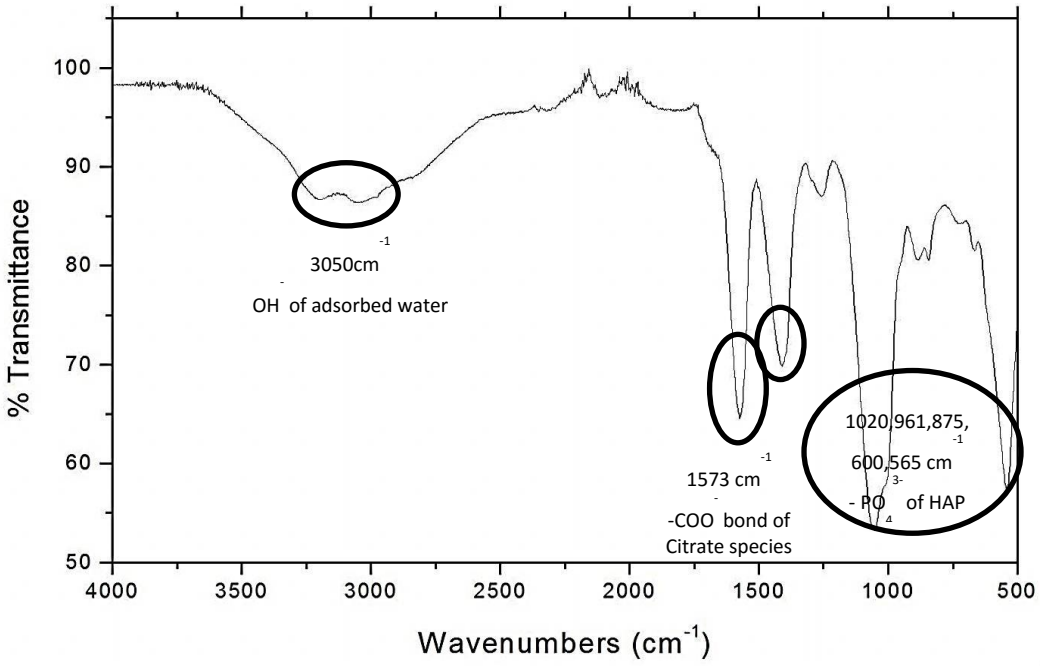

Figure 4.4. FTIR spectra shows calcium phosphate specimens with citrate treatment

4.1.3. FTIR results of calcium phosphate nanoparticles with adjustable crystallinity

FTIR was applied for samples which were air-dried for five days and lyophilized for two days. Some of these samplese were washed with isopropyl alcohol while some were left unwashed. Stretching modes of the OH^- groups corresponding to water at 3300-3400 cm^{-1}, stretching bands at 2360 cm^{-1} and 2330 cm^{-1} corresponding to C=O bond of CO_2 in air composition, bending bands at 876–879 cm^{-1} due to CO_3^{2-} predominantly

belonging to calcium carbonate, and also characteristic peaks of HAP corresponding to PO_4^{3-} at 1010-1100 cm^{-1} and 560-600 cm^{-1} were observed.

FTIR spectra of air-dried-for-seven-days-sample shows the characteristic peaks of hydroxyapatite. Stretching modes of the OH^- groups corresponding to water at 3200 cm^{-1}, and the characteristic peaks of HAP corresponding to PO_4^{-3} at 1015 cm^{-1} and 552 cm^{-1} were observed. In Figure 4.5, FTIR spectra of samples prepared at different drying and washing conditions are shown. No significant difference is seen in the positions of the peaks with respect to the preparation method.

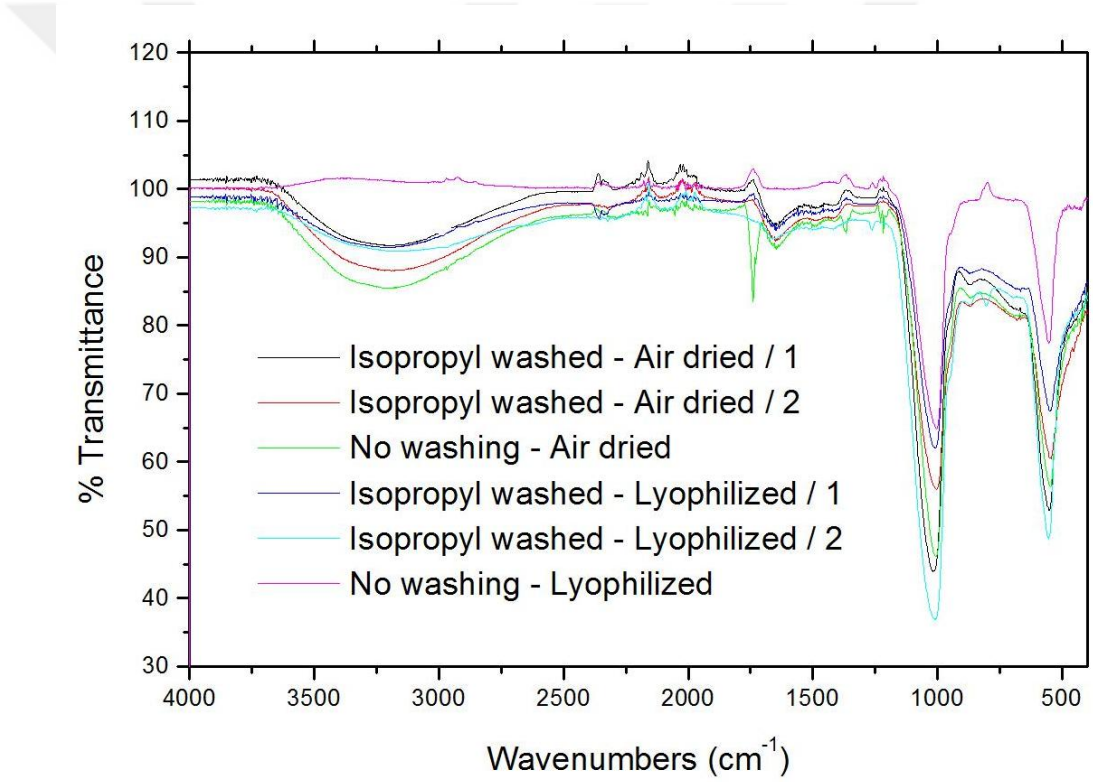

Figure 4.5. FTIR image shows the first measurement of isopropyl washed air-dried HAP samples

As clearly seen above, no difference could be observed about manifested peaks between isopropyl washed/air dried and no washing/air dried samples. But peaks corresponding to groups of HAP are easily visible in all images. For lyophilized samples, peaks that belong to HAP groups are observable in both first and second measurements.

No difference except the absence of wide water peak at 3250 cm^{-1} was found in no washing/ lyophilized samples from others.

4.1.4. FTIR results of hydroxyapatite nanoparticles with polyacrylic acid (PAA) adsorption

FTIR spectra in Figure 4.6 demonstrates the functional groups of PAA (polyacrylic acid-solid sample): OH (2970 cm^{-1}), C=O (1738 cm^{-1}), CH, CH_2 and -CH (1365, 1216, 796 cm^{-1}, respectively).

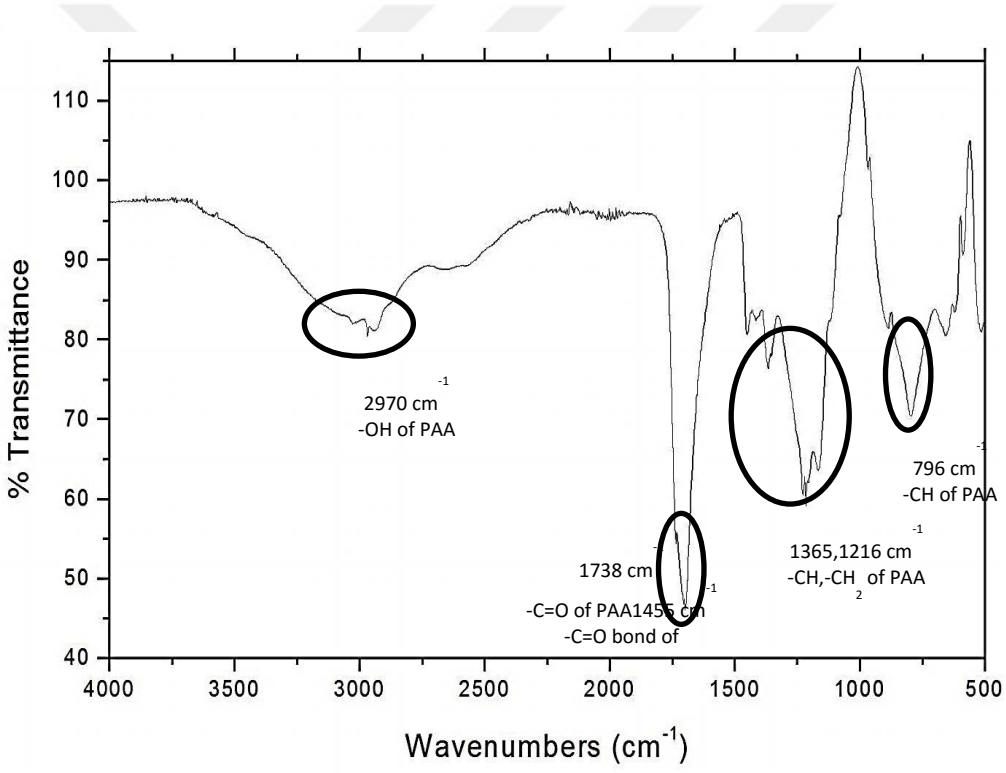

Figure 4.6. FTIR spectra of PAA (solid sample)

Adsorption of polyacrylic acid (PAA) onto hydroxyapatite particles (commercial sample purchased from Sigma-Aldrich) was confirmed with FTIR results shown in Figure 4.6. This sample has no peak for O-H stretching around 3000 cm^{-1}, which demonstrates that there is neither free H_2O nor -OH molecule in this graph. Also hydroxyl groups of hydroxyapatite particles interact with oxygen group of the carboxyl group of PAA through

H-bonding. There is a peak which was observed at 1738 cm^{-1} corresponding to C=O groups of PAA. Additionally, there are few peaks which were detected at 1365-1216 cm^{-1} showing the presence of –CH and -CH_2 groups of PAA. The peaks observed at 1020, 961, 875, 600 and 565 cm^{-1} represent PO_4^{-3} of hydroxyapatite.

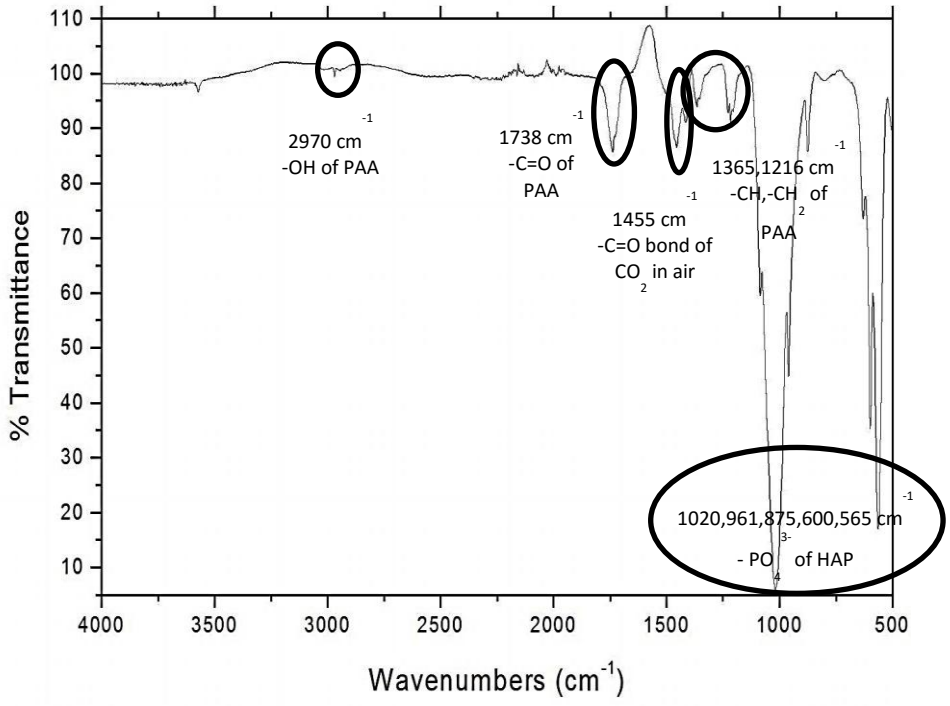

Figure 4.7. FTIR spectra of the 1 mg/ml HAP- 0.25 mg/ml PAA solid sample prepared in ethanol

The FTIR spectra prepared from PAA:HAP of 0.5:1 did not indicate any significant difference with sample of lower concentration (data not shown).

4.1.5. FTIR results of hydroxyapatite nanoparticles with unfunctionalized hyaluronic acid (HYA) and functionalized hyaluronic acid

FTIR characterization was done for the dry-solid samples by using KBr discs.

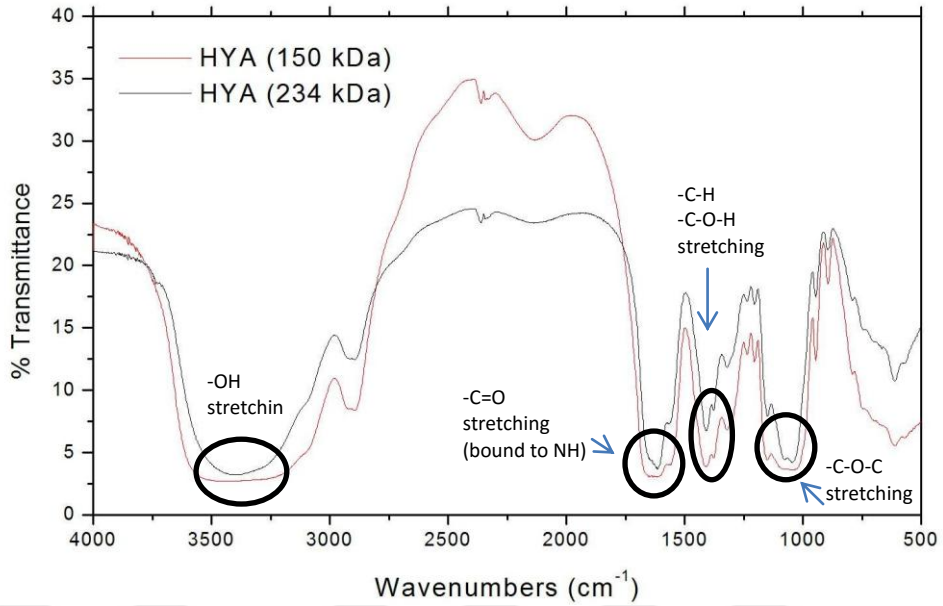

Figure 4.8. FTIR spectra of HYA (pure sample)

Below is the FTIR spectra for hydroxyapatite, functionalized and unfunctionalized hyaluronic acid. FTIR spectra of unfunctionalized HYA includes –OH, -C=O, -C-H, -C-O-H, -C-O-C cm^{-1} stretching bands at 2500-3300 cm^{-1}, ~1700 cm^{-1}, 3000-2850 cm^{-1}, 1100 cm^{-1}, respectively.

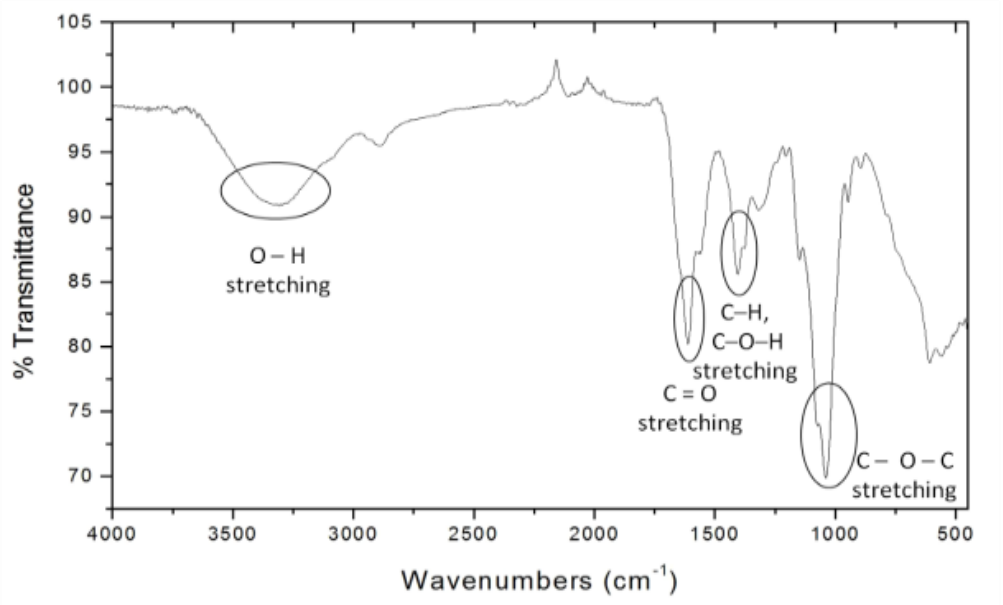

Figure 4.9. FTIR spectra of unfunctionalized HYA (solid sample)

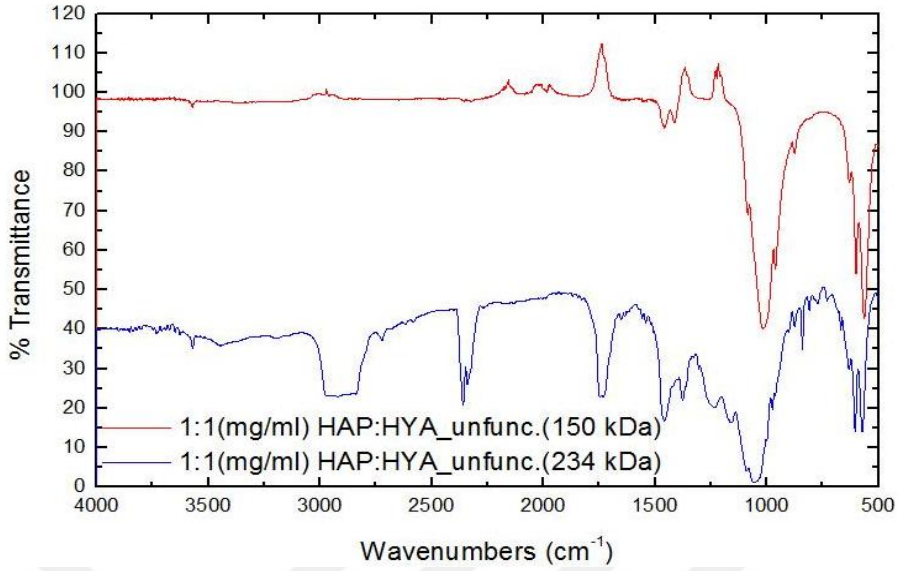

Figure 4.10. FTIR spectra of unfunctionalized HYA (in different molecular weights) adsorbed onto HAP nanoparticles

In Figure 4.11, the characteristic peak of C=C stretching which comes from the aromatic ring of catechol group was clearly seen different from the unfunctionalized HYA.

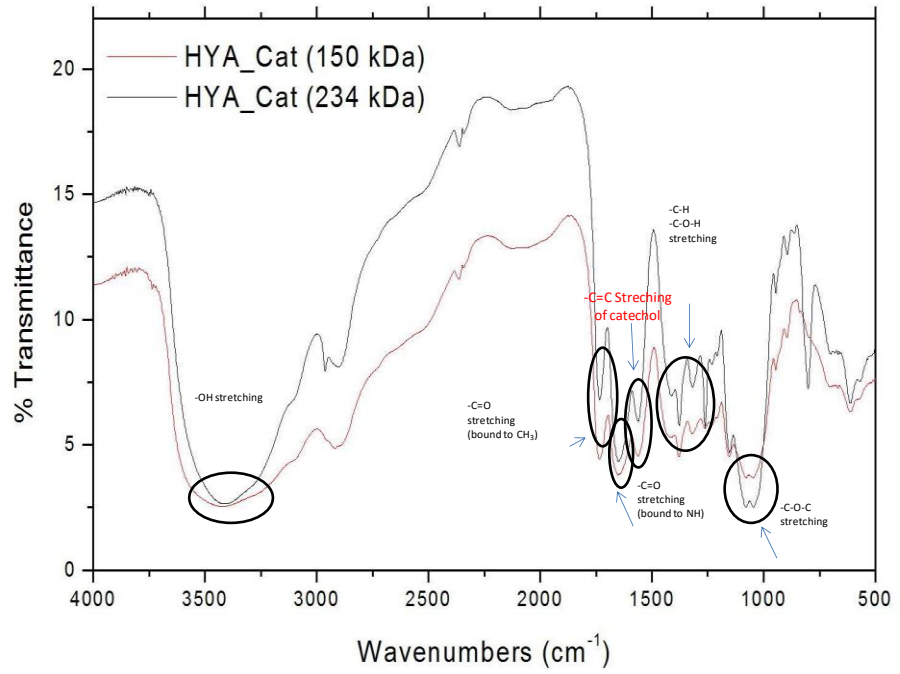

Figure 4.11. FTIR spectra of catechol functionalized HYA (in different molecular weights)

According to Figure 4.12, a few peaks were detected at 3300, 1735-1750, 1050, 1300 cm^{-1} for O-H, C=O, C-O-C, and –C-O-H stretcthing bands, respectively.

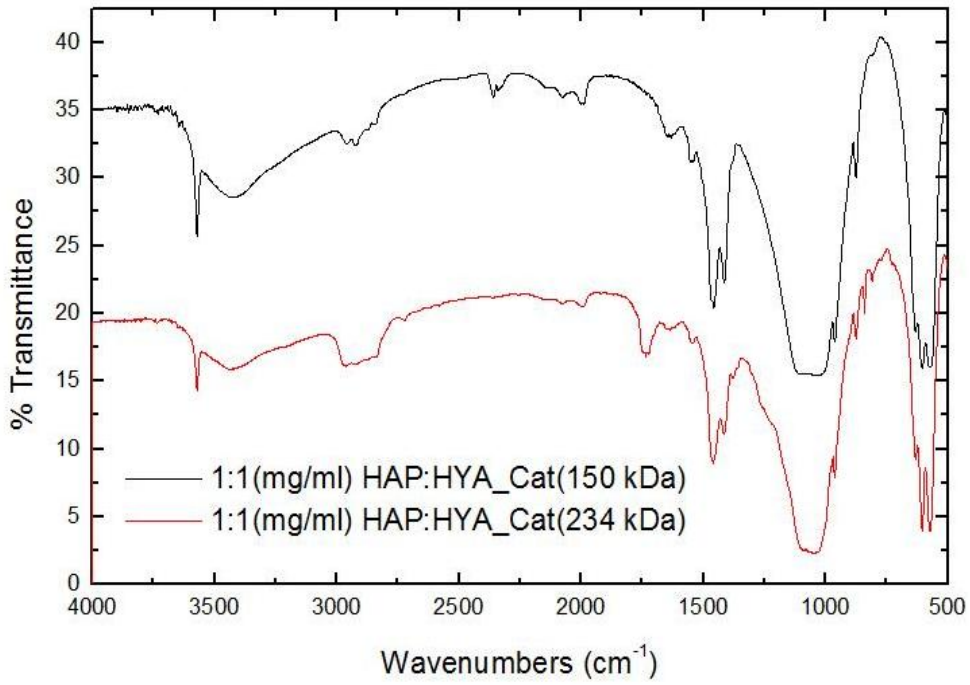

Figure 4.12. Comparable IR spectra of catechol functionalized HYA absorbed onto HAP nanoparticles

4.2. TGA (Thermogravimetric analysis) characterization results for hydroxyapatite nanoparticles with unfunctionalized hyaluronic acid and functionalized hyaluronic acid

TGA analysis was applied for HAP from SIAL, pure HYA and unfunctionalized and catechol-functionalized HYA adsorbed onto HAP.

Also, TGA analysis was done for two solid samples shown below: HAP-unfunctionalized HYA (1 mg/ml HAP - 1 mg/ml HYA) and HAP-unfunctionalized HYA (1 mg/ml HAP - 0.5 mg/ml HYA).

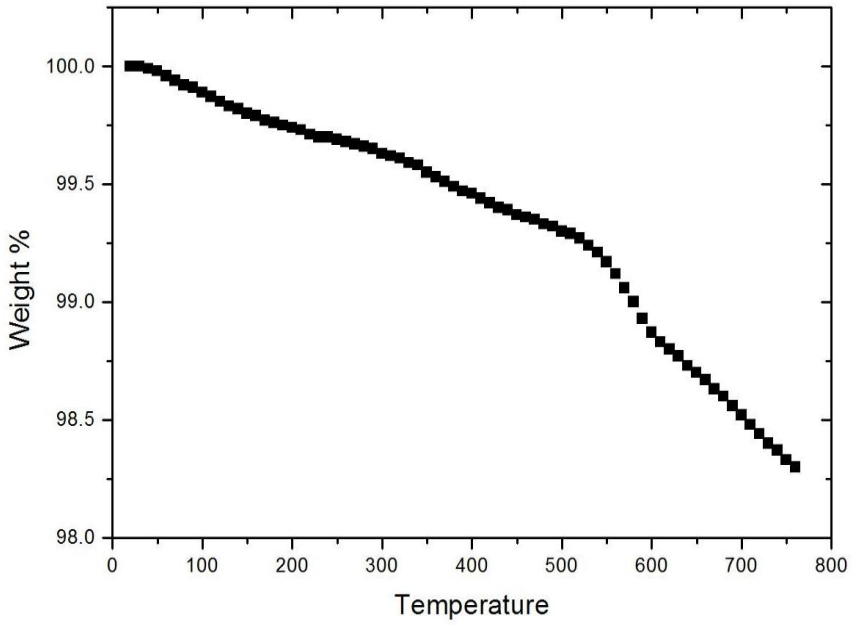

Figure 4.13. TGA analysis of HAP (purchased from SIAL)

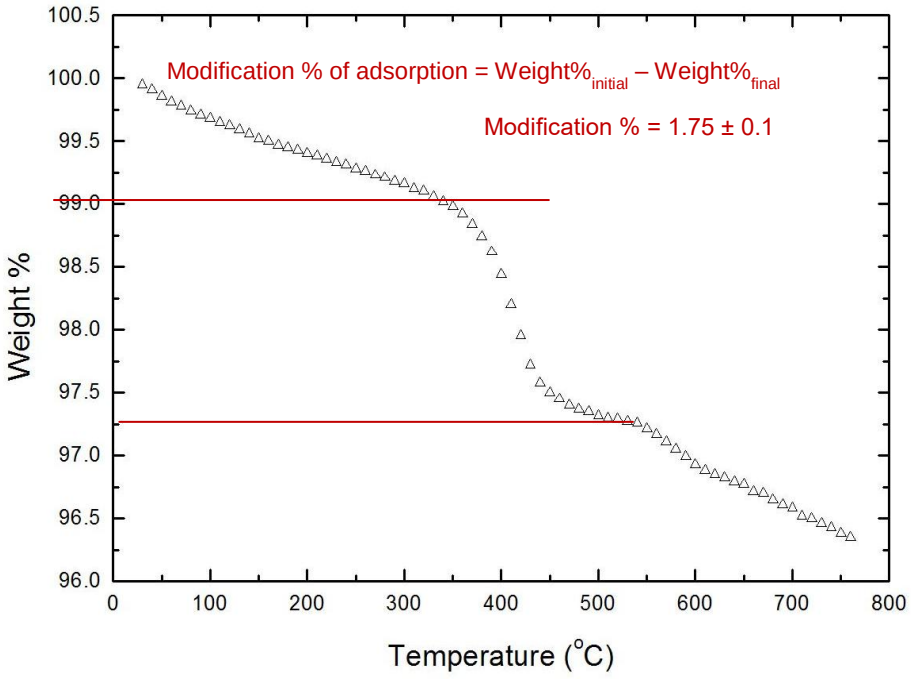

Figure 4.14. TGA data of the 1 mg/ml HAP- 0.25 mg/ml PAA solid sample prepared in ethanol

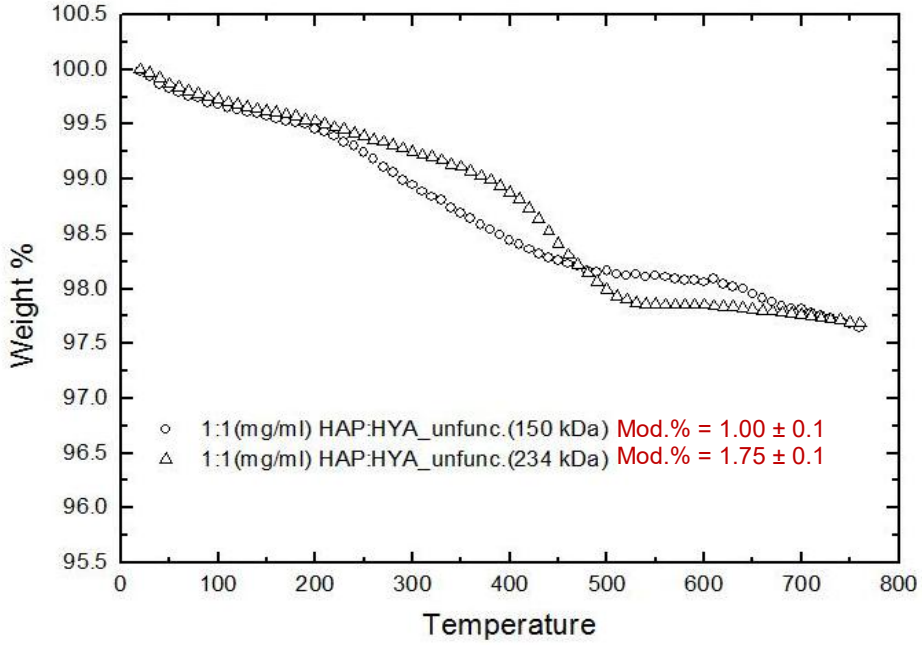

Figure 4.15. TGA analysis of HAP - Unfunctionalized HYA (in different molecular weights)

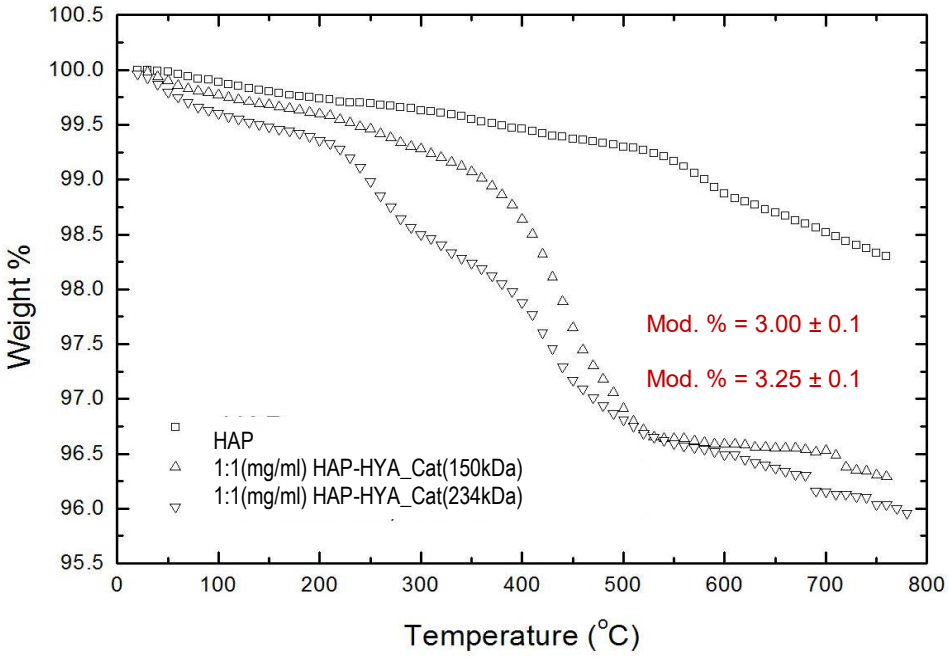

Figure 4.16. TGA analysis of HAP - Catechol functionalized HYA (in different molecular weights)

The results show that the first sample has 1.75 % and the second one has 3% modification. Thus, the results agree with FTIR data that HAP:HYA should be greater than ≥ 2 for efficient modification.

The TGA analysis results for the obtained solid samples are summarized in the Table 4.1 below.

Table 4.1. Summary of the TGA analysis

Concentration of HAP (mg/ml)	Concentration of HYA (mg/ml)	Specialities of HYA	Mod. % of Adsorption onto HAP
1.0	1.0	Unfunctionalized, 150 kDa	1.00 ± 0.1
1.0	1.0	Unfunctionalized, 234 kDa	1.75 ± 0.1
0.5	1.0	Unfunctionalized, 234 kDa	2.75 ± 0.1
1.0	1.0	4.00 % Catechol functionalized, 150 kDa	3.00 ± 0.1
1.0	1.0	4.29 % Catechol functionalized, 234 kDa	3.25 ± 0.1

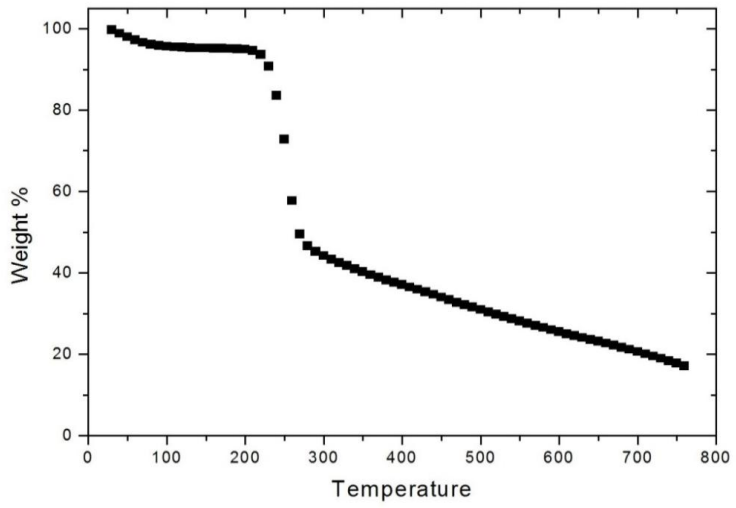

Figure 4.17. TGA data of HYA pure solid sample (150kDa)

4.3. SEM analysis results

The SEM characerization was done for the dried powder sample by covering it with Au in order to obtain a conductive sample. The images below show that the nanoparticles have a diameter of 60-80 nm in length and 25-30 nm in width.

SEM analysis was performed to observe the HAP particules which were prepared wih citrate treatment.

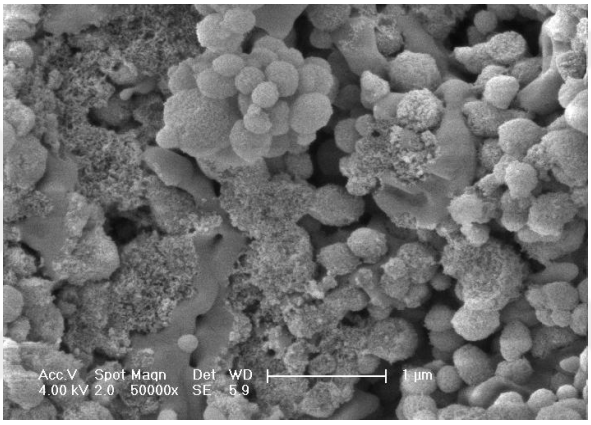

Figure 4.18. SEM image of the HAP particles which were prepared with Kotov's method (1µm)

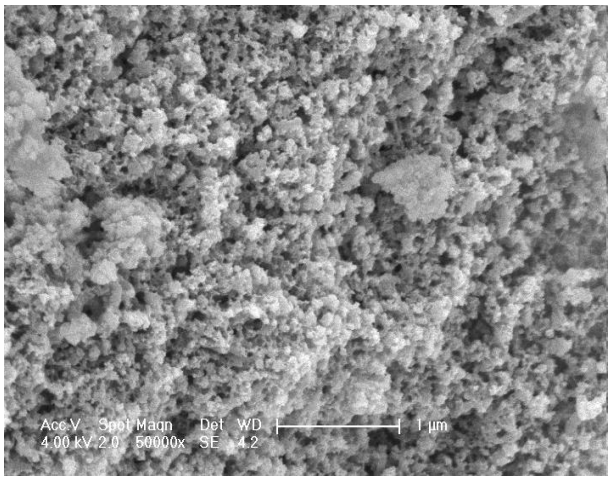

Figure 4.19. SEM image of the HAP particles which were prepared with Costa's method (1µm)

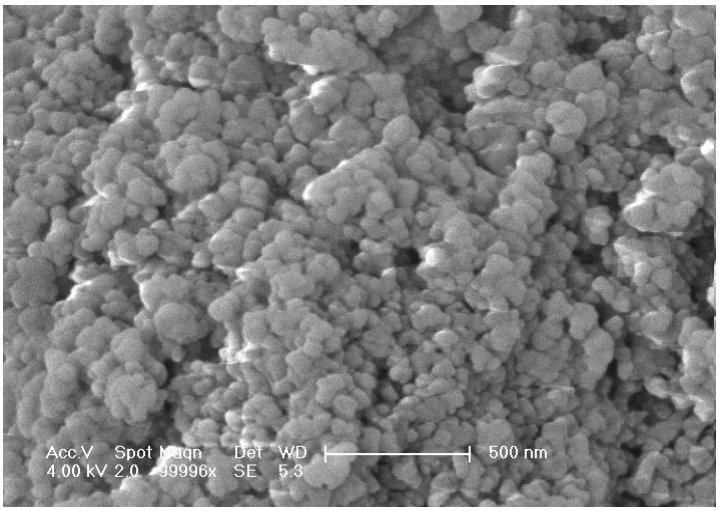

Figure 4.20. SEM image of the HAP particles which were prepared with Epple's method (500 nm)

Table 4.2. SEM Characterization Data of prepared hydroxyapatite particles

Synthesize Method	**Mean (nm)**	**Std. Deviation**	**Yield %**
Kotov's (with CEPA)	145.5	50.9	40
Costa's (Citrate Species)	118.0	36.2	30
Epple's (Nucleation control)	122.9	65.0	85

The HAP particles which were prepared with Costa's and Epple's method were so aggregated that the mean diameters were calculated by looking the small particles into big aggregates.

4.4. XRD Results of Calcium Phosphate Nanoparticles with Treatment of Citrate Species

In order to do the XRD characterization, it is needed at least 0.1 g. And as it is not possible to have enough sample with other two methods, the XRD characterization was just performed for the HAP sample that was synthesized by Costa's method.

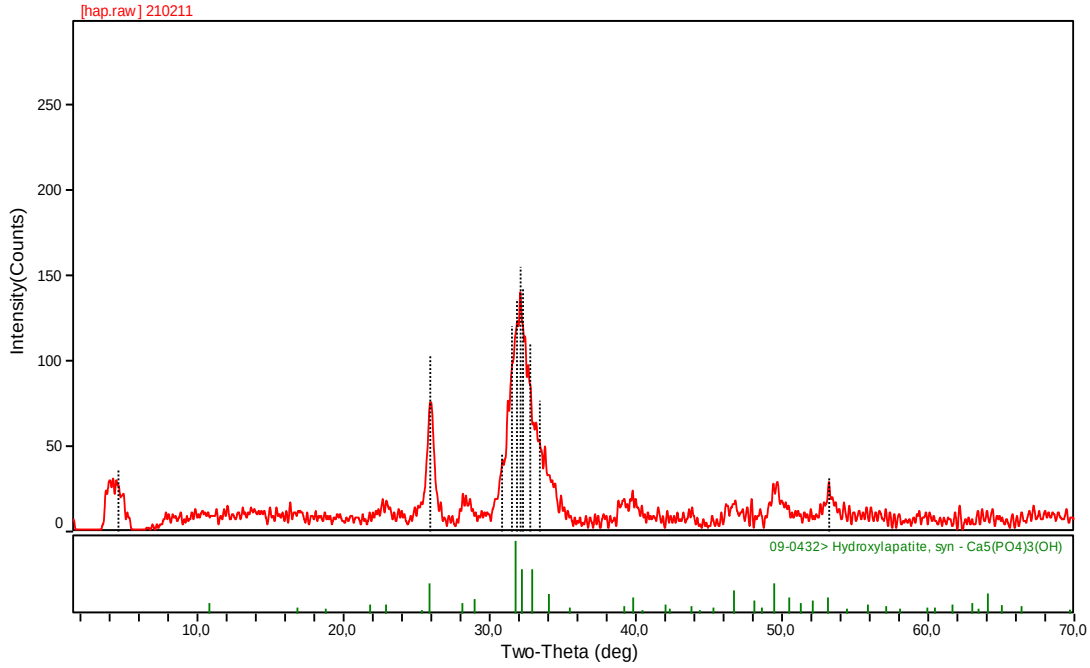

Figure 4.21. XRD image of HAP nanoparticle which was prepared with Costa's method

XRD peaks of synthesized HAP match with the raw datas as shown in the Figure 4.21. The additional peaks and broadening might be due to impurity peaks of HAP.

4.5. DLS Characterization Analysis Results

All samples were filtered w/0.22μm cellulose acetate membrane.

4.5.1. DLS Results of Calcium Phosphate Nanoparticles With CEPA (2-carboxyethylphosphonic acid)

Table 4.3. DLS results of samples that were prepared with Kotov's method

Sample details	d(nm)	G(d)	Solvent	DLS Method
1.09 mg/ml	113.3	23	Milli-Q water	10 run, 1 min.
	136.9	61		
	165.5	100		
	199.9	91		
	241.6	54		
Same sample	100.1	84	Milli-Q water	10 run, 1 min.
after 5 min. of	115.8	100		
sonication	133.9	62		
	154.9	21		

4.5.2. DLS results of calcium phosphate nanoparticles with treatment of citrate species

Table 4.4. DLS results of samples that were prepared with Costa's method

Sample details	d(nm)	G(d)	Solvent	DLS Method
1 mg/ml -	301.0	97	Milli-Q water	10 run, 1 min.
1:5 diluted	322.9	99		
	346.3	100		
	371.3	99		
	398.3	97		
1 mg/ml, stirred	350.2	97	Milli-Q water	10 run, 1 min.
for overnight,	378.2	99		
10 ' sonication	408.1	100		
	440.4	99		
	475.6	97		

4.5.3. DLS results of calcium phosphate nanoparticles with adjustable crystallinity

Table 4.5. DLS results of samples that were prepared with Epple's method

Sample details	d(nm)	G(d)	Solvent	DLS Method
Isopropyl washed, air-dried	187.8 197.8 554.4 583.7	39 41 100 81	Ethanol	10 run, 1 min.
Isopropyl washed, Lyophilized	321.6 350.1 1911.3 2080.6	56 55 100 86	Ethanol	10 run, 1 min.

5. CONCLUSION

The aim of our research in this work was to modify hydroxyapatite (HAP) with catechol-functionalized-hyaluronic acid. Hyaluronic acid (HYA) enables the formation of biologically active scaffolds which can support bone in-growth. We also synthesized three different kinds of HAP: in the presence of 2-carboxyethyl phosphonic acid (CEPA), in the presence of citrate, in controlled the nucleation time following the methods in the literature. However, we ended up using commercial Sigma-Aldrich samples for polymer adsorption studies. In this study, the modification of HAP was accomplished succesfully with catechol-functionalized-hyaluronic acid. As shown in FTIR spectras, modification of HAP was done with HYA in varying amounts of HAP and HYA, and at two different molecular weights of HYA. According to the TGA results, modification percentage of HAP with HYA ranged between 1 and 4%. Highest level of modification, i.e. 3.25%, was obtained for HAP nanoparticles onto which catechol-modified HYA of high molecular weight (234 kDa) was added.

The modification % of HAP nanoparticles is affected by the molecular weight (MW) of HYA, the ratio of HYA to HAP and the functionalization of HYA. If MW increases, modification % of HAP increases for both unfunctionalized and catechol functionalized HYA. As the ratio of HYA to HAP increases, modification % of HAP increases. Also, functionalization of HYA with DOPA-OMe increases the modification % of HAP by 85-300% depending on the molecular weight.

This study can help researchers as a new method for surface modification of hydroxyapatite with polyelectrolytes. Bone-integration of catechol-modified hyaluronic acid which is adsorbed on hydroxyapatite might be the next step for future researchers.

REFERENCES

1. Lian, J., Gorski J. and Ott S., *Bone Structure and Function,* 2004. https://depts.washington.edu/bonebio/ASBMRed/structure.html#BMD, accessed at June 2016.

2. Stagi, S., L. Cavalli, C. Lurato, S. Seminara, M. L. Brandi and M. Martino, "Bone health in children and adolescents: the available imaging technique", *Clinical Cases in Mineral and Bone Metabolism*, Vol. 10, No. 3, p. 166, 2013.

3. LeGeros, R.Z. "Properties of osteoconductive biomaterials: calcium phosphates", *Clinical Orthopaedics and Related Research*, Vol. 395, pp. 81-98, 2002.

4. Dorozhkin, S. and M. Epple, "Biological and Medical Significance of Calcium Phosphates", *Angewandte Chemie International Edition,* Vol. 41, pp. 3130-3146, 2002.

5. Urch, H., M. Vallet-Regi, L. Ruiz, J. M. Gonzalez-Calbet and M. Epple, "Calcium phosphate nanoparticles with adjustable dispersability and crystallinity", *Journal of Materials Chemistry*, Vol. 19, No. 15, pp. 2166-2171, 2009.

6. SofSera Company, *Manufacturing technology of equally sHAPed and sized hydroxyapatite nanoparticle,* 2009. http://sofsera.co.jp/english/tech1_e.html, accessed at June 2016.

7. Uddin, M. H., T. Matsumoto, M. Okazaki, A. Nakahira and T. Sohmura "Biomimetic Fabrication of Apatite Related Biomaterials", *Biomimetics Learning from Nature*, No. 14, 2010.

8. Kovtun, A., R. Heumann and M. Epple, "Calcium phosphate nanoparticles for the transfection of cells", *Biomedical Materials and Engineering,* Vol. 19, No. 2-3, pp. 7-241, 2009.

9. Xingguo, C. and L. Kuhn, "Chemotherapy drug delivery from calcium phosphate nanoparticles", *Int J Nanomedicine,* Vol. 2, No. 4, pp. 667–674, 2007.

10. Al-Sanabani, J.S., A. A. Madfa and F. A. Al-Sanabani, "Application of Calcium Phosphate Materials in Dentistry", *International Journal of Biomaterials,* No. 876132, pp. 1-12, 2013.

11. Sokolova, V., A. Kovtun, O. Prymak and M. Epple, "Functionalisation of calcium phosphate nanoparticles by oligonucleotides and their application for gene silencing", *Journal of Materials Chemistry,* Vol. 17, No. 8, pp. 721-727, 2007.

12. Haedicke, K., D. Kozlova, S. Grafe, U. Teichgraber, M. Epple and I. Hilger, "Multifunctional calcium phosphate nanoparticles for combining near-infrared fluorescence imaging and photodynamic therapy", *Acta Biomaterialia,* No. 10, p. 1016, 2014.

13. Schwiertz, J., A. Wiehe, S. Grafe, B. Gitter and M. Epple, "Calcium phosphate nanoparticles as efficient carriers for photodynamic therapy against cells and bacteria", *Biomaterials,* Vol. 30, No. 19, pp. 31-3324, 2009.

14. LeGeros, R.Z. "Properties of osteoconductive biomaterials: Calcium phosphates", *Clinical Orthopaedics and Related Research,* Vol. 395, pp. 81-98, 2002.

15. Felício-Fernandes, G. and C. M. Laranjeira, “Calcium Phosphate Biomaterials From Marine Algae. Hydrothermal Synthesis And Characterisation”, *Química Nova*, Vol. 23, No. 4, 2000.

16. Wu, S., X. Liu, K. Chu, T. Hu, W. Kelvin, C. Jonathan and X. Zushun, 2012, *Production of three-dimensional hierarchical nano Ti-based metals scaffolds for*

bone tissue grafts, *Handbook of Intelligent Scaffold for Tissue Engineering and Regenerative Medicine,* Edited by Gilson Khang, Pan Stanford Publishing, pp. 69–82.

17. Posner, A.S. and F. Betts, "Synthetic amorphous calcium phosphate and its relation to bone mineral structure", *Accounts of Chemical Research,* No. 8, pp. 81-273, 1975.

18. LeGeros, R.Z., "Properties of osteoconductive biomaterials: calcium phosphates", *Clinical Orthopaedics and Related Research,* No. 395, pp. 81-98, 2002.

19. Sina, Y., "Hydroxyapatite, Chemistry and Processing", *Priciples of Ceramic Processing,* pp. 1-32, 2009.

20. Phirani, J. and K. K. Mohantyb, "Warm water flooding of confined gas hydrate reservoirs", *Chemical Engineering Science,* Vol. 64, No. 10, pp. 2361–2369, 2009.

21. Teraoka, K., A. Ito, K. Onuma, T. Tateishi and S. Tsutsumi, "Bending strength of synthetic OH-carbonated hydroxyapatite single crystals", *Journal of Biomedical Materials Research,* No. 34, pp. 269–272, 1997.

22. Sadat-Shojai, M., M. Khorasani, E. Dinpanah-Khoshdargi and A. Jamshidi, "Synthesis methods for nanosized hydroxyapatite with diverse structures", *Acta Biomaterialia,* No. 9, pp. 7591-7621, 2013.

23. Brundavanam, R. K., G. D. Poinern and D. Fawcett, "Modelling the Crystal Structure of a 30 nm Sized Particle based Hydroxyapatite Powder Synthesised under the Influence of Ultrasound Irradiation from X-ray powder Diffraction Data", *American Journal of Materials Science,* Vol. 3, No. 4, pp. 84-90, 2013.

24. Arsad, M. and P. Lee, "Synthesis and Characterization of Hydroxyapatite Nanoparticles and β-TCP Particles", In: 2011, *2nd International Conference on Biotechnology and Food Science*, IPCBEE vol.7

25. Shaltout, A. A., M. A. Allam and M. A. Moharram, "FTIR spectroscopic, thermal and XRD characterization of hydroxyapatite from new natural sources", *Spectrochim Acta Part A- Molecular and Biomolecular Spectroscopy*, Vol. 83, No. 1, pp. 56-60, 2011.

26. Chandrasekar, A., S. Sagadevan and A. Dakshnamoorthy, "Synthesis and characterization of nano-hydroxyapatite (n-HAP) using the wet chemical technique", *International Journal of Physical Science,* Vol. 8, No. 32, pp. 1639-1645, 2013.

27. Theophanides T., *Infrared Spectroscopy - Materials Science, Engineering and* Technology, InTech, Rijeka and Shangai, 2012.

28. Meejoo, S., W. Maneeprakorn and P. Winotai, "Phase and thermal stability of nanocrystalline hydroxyapatite prepared via microwave heating", *Thermochimica Acta*, No. 447, pp. 115–120, 2006.

29. Ratner, B., A. Hoffman and F. Schoen, *An Introduction to Materials in Medicine, Biomaterials Science, Second Edition*, Academic Press, p. 851, 2004.

30. Raynaud, S., E. Champion and D. Bernache-Assollant, "Calcium phosphate apatite with variable Ca/P atomic ratio I. Synthesis, characterisation and thermal stability of powders", *Biomaterials*, Vol. 23, pp. 1065–1072, 2002.

31. Destainville, A., E. Champion and D. Bernache-Assollante, "Synthesis, characterization and thermal behaviour of apatite tricalcium phosphate", *Materials Chemistry and Physics*, Vol. 80, pp. 269 – 277, 2003.

32. Kwon, S. H., Y. K. Jun, S. H. Hong, "Synthesis and dissolution behaviour of β-TCP and HA/β-TCP composite powders", *Journal of European Ceramic Society*, Vol. 23, pp. 1039–1045, 2003.

33. Mobasherpour, I. and M. Heshajin, “Synthesis of nanocrystalline hydroxyapatite by using precipitation method”, *Journal of Alloys and Compounds,* Vol. 430, pp. 330 – 333, 2007.

34. Han, J. K., H. Y. Song, F. Saito and B. Y. Lee, “Synthesis of high purity nano-sized hydroxyapatite powder by microwave-hydrothermal method”, *Materials Chemistry and Physics*, Vol. 99, pp. 235 – 239, 2006.

35. P. J. Haines, "Principles of Thermal Analysis and Calorimetry", *Royal Society of Chemistry*, Great Britain, Cambridge, 2012.

36. Alqap, A. S. F., S. Adzila, M. Hamdi, S. Ramesh and I. Sopyan, “Thermal Analysis on Hydroxyapatite Synthesis through Mechanochemical Method”, *BIOMED,* Vol. 35, pp. 108–111, 2011.

37. Eslami, H., M. Solati-Hashnjin, F. Bakhshi and M. Tahriri, “Synthesis and characterization of nanocrystalline hydroxyapatite obtained by the wet chemical technique”, *Materials Science-Poland,* Vol. 28, No. 1, pp. 5-13, 2010.

38. Agrawal, K., G. Singh, D. Puri and S. Prakash, “Synthesis and Characterization of Hydroxyapatite Powder by Sol-Gel Method for Biomedical Application”, *Journal of Minerals & Materials Characterization & Engineering,* Vol. 10, No. 8, pp. 727-734, 2011.

39. Alobeedallaha, H., J. L. Ellis, R. Rohanizadehc, H. Costera and F. Dehghania, " Preparation of Nanostructured Hydroxyapatite in Organic Solvents for Clinical Applications", *Trends Biomateri. Artif. Organs,* Vol. 25, No. 1, pp. 12-19, 2011.

40. Camargo, N. H. A, S. Lima and E. Gemelli, “Synthesis and Characterization of Hydroxyapatite/TiO_2n Nanocomposites for Bone Tissue Regeneration”, *American Journal of Biomedical Engineering,* Vol. 2, No. 2, pp. 41-47, 2012.

41. Roeder, R. K., G. L. Converse, R. J. Kane and W. Yue, “Hydroxyapatite-Reinforced Polymer Biocomposites for Synthetic Bone Substitutes”, *Biological Materials Science,* pp. 38-45, 2008.

42. Liu, Q., J. R. Wijn, D. Bakker, M. Toledo and A. Blitterswijk, "Polyacids as bonding agents in hydroxyapatite polyester-ether (PolyactiveTM 30/70) composite", *Journal of Materials Science: Materials in Medicine,* Vol. 9, No. 1, pp. 23-30, 1998.

43. Berret, J. F., N. Schonbeck, F. Gazeau, D. Kharrat, O. Sandre, A. Vacher and M. Airiau, "Controlled clustering of superparamagnetic nanoparticles using block copolymers: design of new contrast agents for magnetic resonance imaging", *Journal of the American Chemical,* 2006.

44. Ishikawa, Y., J. Komotori and M. Sena, “Properties of Hydroxyapatite – Hyaluronic Acid Nano-Composite Sol and its Interaction with Natural Bones and Collagen Fibers”, *Current Nanoscience,* Vol. 2, No. 3, pp. 1-6, 2006.

45. Nemoto, R., L. Wang, M. Aoshima, M. Senna, T. Ikoma and J. Tanaka, "Increasing the crystallinity of hydroxyapatite nanoparticles in composites containing bioaffinitive organic polymers by mechanical stressing", *Journal of the American Ceramic Society,* Vol. 87, No. 6, pp. 1014-1017, 2004.

46. Lee, H. J., H. W. Choi, K. J. Kim and S. C. Lee, "Modification of hydroxyapatite nanosurfaces for enhanced colloidal stability and improved interfacial adhesion in nanocomposites", *Chemistry of materials,* Vol. 18, No. 21, pp. 5111-5118, 2006.

47. Li, C., G. Li, and S. Liu, "Spherical hydroxyapatite with colloidal stability prepared in aqueous solutions containing polymer/surfactant pair", *Colloids and Surfaces A: Physicochemical and Engineering Aspects,* Vol. 366, No. 1, pp. 27-33, 2010.

48. Chirdon, W. M., W. J. O'Brien and R. E. Robertson, "Adsorption of catechol and comparative solutes on hydroxyapatite", *Journal of Biomedical Materials Research Part B: Applied Biomaterials,* Vol. 66, No. 2, pp. 532-538, 2013.

49. Lee, H., S. M. Dellatore, W. M. Miller and P. B. Messersmith, "Mussel-inspired surface chemistry for multifunctional coatings", *Science,* Vol. 318, No. 5849, pp. 426-430, 2007.

50. Chirdon, W.M., W. J. O'Brien and R. E. Robertson, "Adsorption of catechol and comparative solutes on hydroxyapatite", *Journal of Biomedical Materials Research Part B: Applied Biomaterials,* Vol. 66, No. 2, pp. 532-538, 2003.

51. Andres, C., V. Sinani, D. Lee, Y. Gun'ko, N. Kotov, "Anisotropic calcium phosphate nanoparticles coated with 2-carboxyethylphosphonic acid", *Journal of Materials Chemistry,* Vol. 16, No. 40, pp. 3964-3968, 2006.

52. Martins, M. A., C. Santos, M. M. Almeida and M. E. Costa, "Hydroxyapatite micro- and nanoparticles: Nucleation and growth mechanisms in the presence of citrate species", *Journal of Colloid and Interface Science,* Vol. 318, No. 2, pp. 210-216, 2008.

53. Urch, H., M. Vallet-Regi, L. Ruiz, J. M. Gonzalez-Calbet and M. Epple, "Calcium phosphate nanoparticles with adjustable dispersability and crystallinity", *Journal of Materials Chemistry,* Vol. 19, No. 15, pp. 2166-2171, 2009.

54. Çömert F., "Modification of Bioelectrolytes for Bioadhesive Applicaiton", *Graduate Program in Chemistry- Boğaziçi University,* 2012.